

AD-764 267

AN EXPERIMENTAL INVESTIGATION OF THE
EROSIVE CHARACTERISTICS OF 2024
ALUMINUM ALLOY

G. Grant, et al

Cincinnati University
Cincinnati, Ohio

June 1973

DISTRIBUTED BY:

NTIS

National Technical Information Service
U. S. DEPARTMENT OF COMMERCE
5285 Port Royal Road, Springfield Va. 22151

REPORT NO. 73-37

100-10223-5-E



AD 764267

This document is being approved for public release and sale; its distribution is unlimited. The findings in this report are those of the author and are not official Department of Defense policy unless so designated by other appropriate authorities.

AN EXPERIMENTAL INVESTIGATION OF THE EROSIVE CHARACTERISTICS OF 2024 ALUMINUM ALLOY

G. Grant and W. Tabakoff

June 1973

NTIS
NATIONAL TECHNICAL
INFORMATION SERVICE

This work was supported by the U.S. Army Research Office - Durham under Grant Number DA-ARO-D-124-G-154.

31 71

Unclassified

Security Classification

AD-764267

DOCUMENT CONTROL DATA - R & D

(Security classification of title, body of abstract and indexing annotation must be entered when the overall report is classified)

1. ORIGINATING ACTIVITY (Corporate author)

University of Cincinnati

2a. REPORT SECURITY CLASSIFICATION

Unclassified

2b. GROUP

NA

3. REPORT TITLE

An Experimental Investigation of the Erosive Characteristics of
2024 Aluminum Alloy

4. DESCRIPTIVE NOTES (Type of report and inclusive dates)

Technical Report

5. AUTHOR(S) (First name, middle initial, last name)

G. Grant and W. Tabakoff

6. REPORT DATE

June 1973

7a. TOTAL NO. OF PAGES

41 - 48

7b. NO. OF REFS

50

8a. ~~XXXXXXXXXX~~ GRANT NO.DA-ARO-D-~~XXXXXX~~

8b. PROJECT NO.

31-124-71-G154

9. ORIGINATOR'S REPORT NUMBER(S)

Report No. 73-37

9b. OTHER REPORT NO(S) (Any other numbers that may be assigned
this report)

10. DISTRIBUTION STATEMENT

Distribution of this report is unlimited

11. SUPPLEMENTARY NOTES

None

12. SPONSORING MILITARY ACTIVITY

U.S. Army Research Office-Durham
Box CM, Duke Station
Durham, North Carolina

13. ABSTRACT

The erosive characteristics of 2024 aluminum alloy have been experimentally examined. The parameters investigated included the particle approach angle, particle velocity, particle size, specimen length, particle material, particle concentration, and quantity of abrasive impacting the specimen. From this data an analytical model has been developed which will predict the erosion of this material.

Key Words

Erosion

Particulated Flow

DD FORM 1473

REPLACES DD FORM 1473, 1 JAN 64, WHICH IS
OBSOLETE FOR ARMY USE.

Unclassified

Security Classification

REPORT NO. 73-37

AN EXPERIMENTAL INVESTIGATION OF THE EROSIVE
CHARACTERISTICS OF 2024 ALUMINUM ALLOY

G. Grant and W. Tabakoff

June 1973

This work was supported by the U.S. Army
Research Office - Durham under Grant
Number DA-ARO-D-~~31-124-71-G/54~~

31-124-71-G/54

TABLE OF CONTENTS

	<u>Page</u>
LIST OF ILLUSTRATIONS.	ii
NOMENCLATURE	iii
ABSTRACT	iv
INTRODUCTION	1
STATE OF THE ART	2
A. Historical Development.	2
B. Modern Concepts	3
1. Analytical Models	3
2. Empirical Investigations.	8
SCOPE OF THIS RESEARCH.	9
EXPERIMENTAL APPARATUS	10
EROSION RESULTS.	11
A. Effect of Angle of Attack	11
B. Effect of Particle Velocity	12
C. Effect of Particle Size	13
D. Effect of Specimen Width.	13
E. Effect of Particle Material	13
F. Secondary Variables	14
MODEL FOR PREDICTING DUCTILE EROSION	15
A. Erosion at Low Angles of Attack	16
B. Erosion at Normal Impact.	17
C. Prediction of Erosion of 2024 Aluminum Alloy.	18
SUMMARY AND CONCLUSIONS.	20
REFERENCES	21

LIST OF ILLUSTRATIONS

<u>Figure</u>		<u>Page</u>
1	Erosion Test Schematic - Erosion Research Facility.25
2	Test Section - Erosion Research Facility26
3	Test Section Photographic Insert Erosion Research Facility.27
4	Particle Distribution Analyzer - Erosion Research Facility.28
5	Experimental and Predicted Erosion Results.29
6	Effect of Velocity on Erosion Rate30
7	Effect of Velocity on Erosion Rate31
8	Effect of Velocity on Erosion Rate32
9	Effect of Velocity on Erosion Rate33
10	Effect of Particle Diameter on Erosion34
11	Effect of Particle Diameter on Erosion35
12	Effect of Specimen Width on Erosion.36
13	Effect of Particle Mass Concentration on Erosion (MGM/FT^3)37
14	Erosion vs. Quantity of Abrasive Used.38
15	Effect of Normal Component on Tangential Velocity Restitution Ratio39
16	Predicted Erosion for 2024 Aluminum Alloy Impacted by Quartz Sand Dust40
17	Predicted Erosion for 2024 Aluminum Alloy Impacted by Alumina Sand Dust.41

NOMENCLATURE

Symbol

CK	logic operator defining limits of effectiveness of surface ripples
E	quantity of material eroded
K ₁ , K ₁₂ , K ₃	material erosion constants
M	quantity of mass
R	restitution ratio - ratio of conditions before impact to conditions after impact
V	particle velocity
β	angle of impact between particle and target surface
β_0	angle of impact resulting in maximum erosion
ϵ	erosion per unit mass of impacting material

Subscripts

1	conditions of the particle approaching the target material
2	conditions of the particle rebounding from the target material
T	component tangent to the specimen
N	component normal to the specimen

ABSTRACT

The erosive characteristics of 2024 aluminum alloy have been experimentally examined. The parameters investigated included the particle approach angle, particle velocity, particle size, specimen length, particle material, particle concentration, and quantity of abrasive impacting the specimen. From this data an analytical model has been developed which will predict the erosion of this material.

INTRODUCTION

Erosion is defined in this paper as the removal of surface material by a stream of solid particles. The study of erosion may therefore, be divided into two main parts. The first part involves the determination, from the flow conditions, of the number, direction, and velocity of the particles striking the surface. With such information available, the second part of the problem is a calculation of the amount of surface material removed. The first part of the problem, basically, is one of fluid mechanics, and its detailed analysis will not be treated within the scope of this study. However, some aspects of the particle motion in the fluid will be discussed.

As for the second part, that of predicting the quantity of material removed, there is no single theory available to describe the mechanism of material removal. However, most authors do agree that this phenomena can be described for two types of material behavior; namely, ductile and brittle. As empirically distinguished, the "ductile" mode (typical of most metal targets) is characterized by the maximum erosion occurring at an angle less than normal impingement (usually 20-30°). This situation suggests the erosion mechanism might be one of cutting or micromachining, with the sharp corner of the individual particle acting as a miniature single-point machine tool. The "brittle" mode (typical of glasses and ceramics) is characterized by the erosion rate increasing with ascending impingement angle, up to a maximum at normal (90°) impingement. Intuitively this situation suggests the erosion mechanism might be one of constant battering or fatigue of the target surface leading to eventual surface and subsurface cracking and spalling of the material.

Although, for the purpose of this study, the definition of erosion was limited to that caused by solid particles, erosion is also caused by impingement of liquid droplets and cavitation. This type of erosion is similar to that observed in brittle materials impacted by solid particles (i.e. surface and subsurface cracking and eventual spalling of the material), the difference being in the magnitude of the localized stress in the material. Materials exhibiting a poor wear resistance to particle erosion may have a high resistance to cavitation and rain erosion.

A review of the literature indicates that the problem of rain erosion and cavitation has been studied and the basic mechanism elucidated. However, only recently has sand erosion of turbomachines been recognized as a major problem. This has been brought about by the accelerated replacement of erosion-damaged helicopter turbines and compressors in Southeast Asia. Thus, the need exists for a basic understanding of the erosion phenomena in order to establish design criteria. Due to the critical nature of the problem, the present study has been limited to that of solid particle erosion.

STATE OF THE ART

A. Historical Development

A survey of the literature on erosion studies through 1964 was given by Wahl and Hartstein (1). Although there is a wealth of practical information in the many references discussed in this survey, there is little direct information on the mechanism by which the material is removed. This reference indicates that the problem of particles impacting onto different shapes was first studied in Germany (1931) in connection with the collection of smoke and dust particles.

Studies of erosion from a fundamental point of view also appear to have originated in Germany. Siebel and Brockstedt (2) studied the erosion of plates in a stream of quartz sand directed perpendicular to the surface and found that the weight loss of hard or soft steels, as well as alloyed steels, was very much the same. These results were not in agreement with actual experience, for example, pipes of hard steel showed considerable longer life than that of soft steel when transporting abrasive materials. Wellinger (3 to 7) and his co-workers conducted erosion tests at different angles of impingement and clarified this apparent contradiction. They showed that the erosion resistance of different materials could change as the angle of impingement changed. These authors presented their data as a function of the angle of attack and Vicars hardness numbers. This appears to be the first attempt of gathering test data on the process of erosion under a wide variety of controlled conditions. Similar results can be found in the work of Kascheev (8), who eroded a range of copper-aluminum alloys at different angles. At this point, no correlation of the data as related to the physical properties of the material was attempted.

In 1949 R.L. Stoker (9) described the different behavior of brittle (Gypsum) and ductile (Black Iron) materials as to the effect of erosion rate and angle of attack. The basic purpose of his tests was to investigate the possibility of using plaster models for predicting the erosion life of more durable materials. Stauffer (10) attempted to standardize the erosion data by whirling 3 different test specimens in a slurry and comparing their erosion to a fourth specimen which was designated as a standard. One interesting result to be obtained from his data (and apparently overlooked by the investigator) is the completely different behavior of the erosion pattern when the material hardness exceeded that of the particle hardness. Stauffer also investigated the effects of surface hardness. As might be expected, sprayed or electroplated coatings did little to reduce erosion.

Finnie (11, 12, 13), employing photographic techniques and a high speed light source, was the first to measure the speeds of the erosive particles. He found that the weight loss of an annealed steel target (ductile) was proportional to the square of the speed of the eroding particles. Properties of the erosive agents considered important were particle size, shape, hardness and strength.

As a consequence of these studies, Finnie developed the initial mathematical model for predicting erosion of ductile materials. In this model he assumed that the particle cut through the material as the localized stress reached the plastic flow stress (assumed constant). By considering the behavior of a single abrasive grain impinging on the surface, equations were derived which predict the weight loss by erosion.

The results of this model compared favorably with the experimental data obtained, at least until the angle of maximum erosion was reached. The model predicted no erosion would occur at normal impingement, which was contrary to experimental evidence. An empirical correction factor was used to improve the predictive ability of the model. The correction was justified by assuming that the particles striking the surface after some erosion had occurred, see a roughened surface, and thus, the cutting angle may be acute to the local micro-surface.

Finnie indicated that it would be very difficult to predict the erosion of brittle targets because of the complex nature of the origin and growth of fracture in such materials.

B. Modern Concepts

1. Analytical Models

In the literature previously described, most of the basic parameters and concepts of solid particle erosion were discussed. However, except for the model described by Finnie (13), there was no attempt to develop a quantitative tool to predict the erosion. In more recent years (1960 to present) activity into this field was stimulated due to the increased dependance on gas turbines. The following is a brief description of the most important literature published during this period.

Finnie (13) proposed equations of motion for angular particles cutting through a ductile target surface. The basic equation attempts to predict erosion weight (loss per individual dust particle collision) as being directly proportional to the total Kinetic energy of the particle and inversely proportional to the minimum flow stress of the target material, or

$$\text{Erosion loss} = C f(\beta_1) \frac{M V_1^2}{p}$$

where:

C = constant for specific erosion system

$f(\beta_1)$ = function of incidence angle (β_1)

M = dust particle's mass

V_1 = dust particle's approach velocity

p = minimum flow stress of target material surface at test temperature.

Hence, the higher the material's flow stress, the greater its resistance to micromachining forces and thus the smaller the chip formed. As was mentioned previously, Finnie's equation did not correctly predict the erosion near normal impact. Thus, to obtain a better fit for the experimental data, Bitter (14,15) modified Finnie's original equation as follows:

$$Q = \frac{1}{2} \frac{M(V_1 \sin \beta_1 - k)^2}{\lambda}$$

where:

Q = erosion in units of volume lost

M = total mass of eroding particle

k = constant, related to threshold velocity below which erosion stops

λ = energy needed to remove a unit volume of target material (repeated deformation wear).

He also defined two types of wear, these being wear due to repeated deformation (W_d) and cutting wear (W_c). The equation presented above is for deformation wear, which results from the repeated impacts suffered by the specimen and which eventually causes cracking and spalling of the material. Deformation wear causes the erosion for normal impingement in ductile materials and is not accounted for in Finnie's analysis.

Bitter's work takes into account the elastic as well as the plastic properties of the particle and specimen materials. The complexity of Bitter's final relationship prompted Neilson and Gilchrist (16) to propose a somewhat simpler set of equations as follows.

$$Q = \frac{\frac{1}{2} M(V_1^2 \cos^2 \beta_1 - V_{2p}^2)}{\phi} + \frac{\frac{1}{2} M(V_1 \sin \beta_1 - k)^2}{\lambda}$$

where the nomenclature is the same as that of Bitter's equation with the addition of:

V_{2p} = Residual horizontal component of particle velocity (this term becomes increasingly significant with decreasing impingement angle)

ϕ = Energy needed to remove a unit volume of target material (cutting wear).

The first term on the right side of the equation represents the cutting wear and the second term accounts for the deformation wear.

Both Bitter and Neilson and Gilchrist recognized the need to include threshold conditions. Neilson and Gilchrist's major contribution was the assumption that total erosion is the arithmetic combination of brittle and ductile contributions, and thus erosion loss can be predicted at intermediate impingement angles. However, the resulting equations are still very complex to work with due to the difficulty in measuring quantities such as ϵ , k , V_{2p} and ϕ .

Another analysis of the erosion problem was conducted by Finnie and Kabil (17). They explained the regular ripple pattern which forms when ductile materials are eroded at angles at or near that for maximum volume removal in terms of the plastic flowing action of the materials.

Sheldon and Finnie (18) discarded the idea of predicting volume removal on an energy basis in their investigation of the behavior of brittle targets subjected to homogeneous erosive agents. They found good correlation between the amount of erosion produced by particles impacting normal to the surface and a statistical description of the strength of brittle materials, the Weibull flaw parameter. The volume of material removed by a given number of particles was predicted to be;

$$Q = k r^{f_1(m)} V_1^{f_2(m)}$$

where:

Q = volume of material removed

k = a quantity involving material constants

r = radius of a sphere with weight equal to the particle

$f_1, f_2(m)$ = prescribed functions of m , the flaw parameter of the Weibull fracture strength distribution.

Head and Harr (19) concluded that even though the previous analysis correctly identified the parametric relationships involved in erosion, they were of little value when the contaminant was not homogeneous. They chose to describe the data in a statistical manner. The parametric relationship used in their analysis was determined using the Buckingham Pi theorem, to be:

$$A = \frac{V^2}{E} f(R, \beta, \frac{H}{E}, \frac{B}{E})$$

where:

- A = erosion rate (ft³ of material eroded/lbm of particles)
- V = the "effective" velocity of the mixture
- E = erosion resistance
- R = "effective" roundness of particles
- H = "effective" hardness of the dust
- B = hardness of the target.

By analyzing the available data using the above relationship in conjunction with a linear regression analysis program, the following equation was expressed for ductile targets:

$$A = \frac{(V^2/E)^{2.17} \quad 0.46 \quad (H/E)^{0.10}}{R^{2.84} \quad (B/E)^{2.48}}$$

The model that these authors proposed for brittle materials did not adequately describe the experimental data.

Smeltzer et.al. (20), proposed a unique model of erosion based upon highly magnified observations of the impression an incoming particle (of given size and velocity) makes on a target surface. The mechanism of material removal was assumed to consist of two components. The first component, called Mechanism 1, characterizes the erosion due to localized melting followed by partial splattering. Mechanism 2 accounts for the material removal due to the process of localized melting, partial adherence or bounding to the particle, and subsequent dislodgement by later impacts. The results were expressed in terms of the following set of equations:

$$W_{R_1} = \eta \phi(90 \text{ degrees}) \sin \beta_1 (1 - \sin \beta_1) \left[\frac{1}{2} \frac{MV_1^2}{F} \right]$$

$$W_{R_2} = \zeta \phi(90 \text{ degrees}) \sin^2 \beta_1 \left[\frac{1}{2} \frac{MV_1^2}{F} \right]$$

and $W_R = W_{R_1} + W_{R_2}$

where

- W_{R_1} = quantity of material removed by Mechanism 1
- W_{R_2} = quantity of material removed by Mechanism 2

W_R = total weight of material eroded

$\phi(90 \text{ degrees})$ = Probability that a particle impacting the plate at 90 degrees will be "snagged" by the target

η = fraction of splattered material that actually escapes

ζ = fraction of material dislodged by Mechanism 2 that actually escapes

M = mass of the particles

F = energy required to melt 1 gram of target material

Sheldon and Kanhere (21) observed the damage caused by the impact of a relatively large single particle on an aluminum surface. They then developed a model similar to that presented earlier by Goodier (22). The particle penetration equation was based on indentation hardness theory, where the strain hardening and inertia of the impacted surface were not considered. This model best describes the physical mechanism of erosion, as the basic hypothesis proposes that the material removed by the impacting particle is not cut out as a chip, but rather flows around the sides of the cavity until the displaced material is strained sufficiently to break off. The final result indicated that the material removal, E , of particles of a fixed size would be proportional to:

$$E \propto q^3 = \frac{D^3 V^3 (\rho_p)^{3/2}}{H_v^{3/2}}$$

where:

q = maximum penetration depth of the particle

H_v = vicars diamond pyramid hardness number

D = particle diameter

V = particle velocity

ρ_p = particle density.

This model, which accounts for the properties of the particle as well as those of the target material, was the first that predicted that erosion can have a velocity dependence greater than 2.

The analytical methods previously obtained to describe the erosion process have primarily been developed from two viewpoints. Some investigators have used a predominatly empirical approach that

usually involves a basic assumption as to the process governing material removal together with the introduction of a parameter such that the proposed relations would fit the test data (14,15,16, 19 and 20). The merit of this approach is that it provides a systematic means of grouping materials and for correlating experimental results, but it offers limited understanding of the material behavior itself.

The other approach to predict erosion behavior of materials is one that may be described as a more conventional type of analysis problem. It consists of considering the dynamic forces between the surface and the particle and predicting the volume removal from well-known material properties. The use of this approach is straightforward; the main difficulties occur because of the unknown condition of the material during impact, which necessitates that some assumptions be made. This approach has been used in analyzing erosion behavior of both materials which can be assumed to behave in a ductile manner and of materials which behave in a brittle manner (13,17, 18 and 21).

Some investigators have proposed a third approach to the analysis of the erosion problem. In this analysis it is assumed that the material behavior during erosion is unique and that there exists no common material property such as hardness or modulus of elasticity that can be used in describing the action of the surface under impinging particles. Thus, Thiruvengadam (23) uses a quantity called erosion strength to relate the erosion resistance of a large variety of engineering materials to the energy absorbed by the material. Kriegel (25) introduces a quantity called wear stress in his derivation for erosion wear rate. This quantity, wear stress, is not entirely unique, but is a function of the yield strength and the fracture strength of the material.

The one conclusion that can be made after reviewing the various analytical studies made to date, is that there is no universally acceptable method of predicting erosion, even for the simplest of geometric configurations.

2. Empirical Investigations

The remainder of the literature reviewed can be divided into two categories; i.e., a discussion of specific industrial erosion occurrences and the results of experimental investigations. Erosion has been reported as a problem in areas as diverse as aero-gas turbines (25 to 33), rocket nozzles (34), transport tubes (1, 10 and 13), coal fired boiler systems (35) and scale removal equipment (9). However, the most severe problem reported appears to be the operation of gas turbine powered vehicles over dust terrains.

This review indicates that although the basic mechanisms of erosion are not yet fully elucidated, the majority of parameters effecting erosion have been investigated in some detail. It has been well established that the quantity of material eroded, E , is primarily a function of the mass of the particles impacting, M , the impacting particle velocity, V_1 , and the inbound angle of attack,

§1. Other variables such as dust concentration, stress concentration, particle size, temperature, erosion threshold and aerodynamic environment are considered as secondary variables because of their relatively small affect on the erosion damage (ϵ).

Several authors have investigated the the mechanisms of brittle material erosion (14,18,37 and 38) and their results have validated the model proposed for this mode of erosion (i.e. that of fatigue failure accompanied by surface and subsurface cracks). Since the materials subjected to erosion in gas turbines are predominantly ductile, it is logical that these materials would receive more attention in the literature (13,15,19,36 and 39 to 47). From these results, it has been fairly well established that considering the material removal mechanism as being a plastic flow action enables the observed experimental results to be accurately described. However, no authentication of the micromachining hypothesis exists.

SCOPE OF THIS RESEARCH

The literature search previously described indicates that the mechanisms of erosion have been investigated primarily from an empirical viewpoint, with this information then being utilized to establish the requisites for an erosion resistant material. Although this approach is a valid one, most engineering problems must also consider many other criteria. For example, the choice of materials in a gas turbine are dictated by a series of trade offs made by a design engineer who may not consider erosion as being an important criteria. If erosive strength is an important design criteria, the designer can predict the effect it will have on performance and weight. However, no tool exists which will help him to predict the gain in life resulting from his consideration of erosion, short of a full scale destruction test under the prescribed conditions.

It is apparent that if erosion is to be considered as an important criteria in the design of gas turbines, it will be necessary to develop a model which will predict the quantity of erosion that a part undergoes in a designated environment. In conjunction with this, the erosion profile is necessary to relate erosion to the life of the part. Only then can the costs of the increased maintenance or filtering be traded off with the other important parameters of gas turbine design.

A very complex computer model is presently being developed to estimate the erosion in rotating machinery. However, in order to make this model operational, two complete sets of empirical data are needed. The first set of data required is the impact and rebound characteristics of high speed particles. This is necessary because the particle trajectory must be traced through a flow field after multiple high speed impacts. This information has been obtained for quartz particles impacting on 2024 aluminum alloy and is reported by the authors in Ref. 48. The other set of data required

is, of course, the quantity of erosion that will be removed at impact. The purpose of this report is to present the results of an extensive investigation of the erosive characteristics of 2024 aluminum alloy being impacted by alumina and quartz particles. From this data, the required predictive model of erosion, for this combination of materials, will be developed.

EXPERIMENTAL APPARATUS

A specially designed wind tunnel was constructed to obtain the basic erosion data and to photograph the particle impacts. A detailed description of this facility, along with design drawings are found in Reference 49. The main considerations in designing the test equipment were to control the primary variables of fluid velocity, particle velocity, particle flow rate, and particle size in a representative aerodynamic environment. Provisions were also made to vary the angle of attack between the abrasive particle and the surface of the test specimen.

Figure 1 is a schematic of the apparatus which fulfills these objectives. As depicted in this illustration, the equipment functions as follows.

A measured amount of abrasive grit of a given consistency is placed into the particle feeder, A. The particles are fed into a secondary air source which carries them to the particle injector, C, where they mix with the main air supply, B. The particles are then accelerated by the high velocity air in a constant area duct, D, and impact the specimen in the test section, E. The test dust is then separated from the air by a cyclone separator, G, and collected in a container, H. The test air is then filtered through a commercial 5 μ filter, F.

The test section was designed such that the experiments can be run in a rapid manner without destroying the aerodynamic parameters. The basic geometry of the test section is illustrated in Figure 2. From this figure it may be observed that the tunnel geometry is uninterrupted from the acceleration tunnel into the test section. Hence, the particle laden air is channeled over the specimen while the aerodynamic characteristics of the fluid passing over the blade at the given angle of attack are preserved. In order to minimize the tunnel blockage, three different sized specimens were used. At angles of attack of 0 to 20 degrees a one inch wide specimen was used, from 20 to 45 degrees, a one-half inch wide specimen is used and for large angles of attack of 45 to 90 degrees, a one-fourth inch wide specimen was used. In this manner, the maximum tunnel blockage is on the order of 10%.

The test section was constructed with several different inserts to obtain all of the required data. Figure 2 illustrates the basic

test section geometry and the test specimen holder. The channel geometry is the same as that of the acceleration section, that is 3 inches x 1 inch at the location of the specimen, the channel turns 30 degrees. Figure 3 illustrates the photographic insert through which high speed photography and streak photographs were taken of the sand particles. This insert consists of an enclosure plate, a replaceable glass insert, and a collar to hold the insert. The high speed particles scratch the glass through which the pictures are taken, and thus, is replaced after each test. This unique test facility has resulted in very high quality pictures without disrupting the flow field.

The test section design is inefficient in one manner, as only a small percentage of the particles that are introduced into the fluid stream impact on the specimen. This, of course, is necessary to preserve the aerodynamic characteristics over the blade. The main concern that arises when using a testing apparatus of this type is that the particle distribution in the tunnel may not be uniform, and thus the predicted amount of particles impacting the plate may not be accurate. To investigate this problem a final section was designed. This section, which is illustrated in Figure 4, divides the channel into 24, $3/8 \times 1/3$ inch sections, and ducts the particulated mixture through a collection tube and then into a filter bag. By weighing these filter bags before and after a test, the particle distribution in the tunnel can be determined.

EROSION RESULTS

The erosion test facility, described previously, was designed in such a manner that the erosion could be measured without destroying the aerodynamic environment. Care was also taken to insure that the surface finishes of the specimens were similar prior to testing. The erosion was determined by measuring the weight of the specimen before and after testing. The abrasives used were alumina (Al_2O_3) and quartz (SiO_2) obtained from commercial suppliers.

Parameters such as angle of attack, particle velocity, and duration of erosion can strongly influence the extent of the erosion damage, and hence, received close attention in this study. Other parameters such as particle concentration, particle diameter, and specimen configuration have been tested sufficiently to determine the effect, if any, that they will have on the result.

A. Effect of Angle of Attack

One of the more interesting features of erosion of ductile materials is the manner in which the angle at which the particles strike the target surface influences the metal removal rate. Figure 5 illustrates this relationship for 2024 aluminum alloy. This figure summarizes the results obtained for different velocities. For

the conditions studied, the angle of maximum weight loss occurs at an angle of approximately 20 degrees. As the angle of attack increases from this value, the erosion reduces to a residual value at 90 degrees. This relationship is very unusual and has been the subject of much analysis. Finnie's analysis (11), which considered the particle as a single pointed cutting tool, adequately predicted erosion at low angles of attack but predicted zero erosion at normal impact. Bitter (14,15) hypothesized that two mechanisms are involved in the erosion process. The first of these is associated with scratching or shearing as described by Finnie. The second is associated with a repeated deformation phenomenon similar to a fatigue spalling. This mechanism is not substantiated by photomicrographs of the impacted surface. Instead, it appeared that the impacts caused extensive surface flow and plastic deformation at all angles of attack.

The experimental results obtained and presented in Figure 5 indicate that the effect of the angle of attack is independent of particle velocity. However, the definition of the point of maximum erosion becomes much more explicit with increasing velocity.

B. Effect of Particle Velocity

The early investigators of erosion proposed that the process was proportional to the kinetic energy of the oncoming particle. This predicted relationship (i.e., $\epsilon \sim V^2$) would almost intuitively be expected from kinetic energy considerations. However, experimental observations have shown that the velocity exponent could be greater than two. Finnie et.al. (39) found that a velocity exponent as high as three could be expected if cutting depth of the particle is assumed as a function of the material strength. Tilly and Sage (46) proposed that the velocity exponent is greater than two as a result of particle fragmentation upon impact, since the particle fragments flowing over the eroded surface cause secondary damage. Finally, Sheldon and Kanhere (21) developed a particle penetration equation based on indentation hardness theory which predicts that the velocity exponent may be as high as three. Despite these analyses, the exact reason for the velocity exponent being greater than two is perhaps the single most controversial issue in the study of erosion.

The effect of velocity was investigated at angles of attack of 20 degrees and 90 degrees. These results are presented in Figures 6, 7, 8 and 9. The influence at the other angles of attack is illustrated in Figure 5. The data for 20 degree impact (Figures 6 and 8) indicates that the velocity exponent is approximately 2.8 for both the alumina and quartz sand particles (i.e., $\epsilon \sim V^{2.8}$). At normal, or 90 degree impact, the velocity exponent is 4. Again, as can be seen from Figures 7 and 9, this functional relationship is the same for both quartz and alumina particles. To the knowledge of the author, this is the highest velocity exponent found in the literature. This may be due to the inclusion of the aerodynamic effects in the test facility. The smaller alumina particles deviate from the general trend of the data as the velocity increases. This

could be a result of these particles actually penetrating the specimen and adhering to it, thereby adding to the specimen weight. Other than this, the particle size does not influence the parametric relationship between velocity and erosion.

C. Effect of Particle Size

It has been found that particle size can influence the rate of erosion. This parameter is plotted in Figures 10 and 11 for alumina particles at two different angles of attack; 20 and 90 degrees. These data indicate that the erosion damage increases with particle size up to some plateau value.

Further, the influence of particle size on erosion is more pronounced at higher particle velocities. It is felt that this phenomenon is primarily a result of the particles imbedding themselves into the specimen material, thus increasing the specimen weight as mentioned previously.

D. Effect of Specimen Width

A very interesting result of this research was the manner in which the width of the specimen influence the erosion rate. The specimen used was one inch in length and it was placed in a 1 inch by 3 inch tunnel. The width of the specimen was determined by the consideration of tunnel blockage. If the specimen was very wide, it would block a large amount of the tunnel flow area and significantly alter the aerodynamics in the test section. However, if the tunnel blockage was too small, very large quantities of sand would be required in order to have sufficient quantities of the particle material impacting on the specimen. Thus, it was decided to change the width of the specimen from 1/4 inch to 1/2 inch and finally to 1 inch as the angle of attack was reduced. In this manner, the blockage was maintained at approximately 10%. The results of this change indicate that the width of the specimen itself influenced the erosion rate. Each time the specimen width was increased, the erosion rate dropped. This phenomena appears to be independent of particle size, particle diameter, particle material, angle of attack, and quantity of mass impacting the specimen and is dramatically depicted on Figure 12. This result could be caused by an aerodynamic pitching moment of the longer particles making an unfavorable orientation of the cutting edge. At this time, however, it is felt that more research is required into this area to determine the exact mechanism.

E. Effect of Particle Material

Although this parameter was not studied in any great depth, two different particle materials were used in this research, these being alumina and silica. The material of the particle can markedly influence the severity of the erosion. This can be directly related

to the hardness and the sharpness of the material. In nature these two properties are inter-related, as a soft material is usually more rounded than a hard material.

The erosiveness of alumina, as determined from this research, is approximately 50 percent greater than that of quartz. These dramatic results are very important in the commercial applications of erosion. However, natural dusts contain a range of geological constituents of which quartz is usually the most common as well as the most erosive material present (43). Thus, these results are only of academic importance when investigating the erosion mechanisms in natural environments.

F. Secondary Variables

Other parameters investigated were the particle concentration, the quantity of abrasive used, and the particle distribution within the tunnel. These variables are listed as secondary since they have a relatively small effect on the erosion mass parameter.

The dust concentration effects were measured using 80 micron alumina dust impacting at an angle of 30 degrees. The erosion that occurs over a large range of dust concentrations is plotted in Figure 13 for two different particle velocities. It is evident from this plot that erosion efficiency does not vary in any appreciable manner with the magnitude of the dust concentration.

A series of tests were conducted to determine if the quantity of mass impacting on the specimen will influence the resulting erosion rate. The results of these tests are plotted in Figure 14. The results show that the quantity of material removed from a surface by erosion is almost linearly proportional to the mass of the particles that impacted upon that surface.

As was previously mentioned, the test section was designed in such a manner that approximately 10 percent of the particulated flow impacted the specimens. To determine the uniformity of particle distribution in the tunnel, tests were conducted for particle velocities (450 ft/sec and 550 ft/sec) and a large and small particle size (200 microns and 50 microns). Each test gave identical results, as it was found that the particle concentration in the region impacting the specimen was approximately 3 percent higher than the average particle concentration. Other than this small variation, the particle concentration was very flat with the lowest concentration existing in the corners of the tunnel. The three percent variation was taken into account in the analyses of the erosion data.

MODEL FOR PREDICTING DUCTILE EROSION

Erosion data on 2024 aluminum alloy indicates that the particle velocity influences the amount of material removed to a greater degree than might be expected from strictly kinetic energy considerations. This result has been verified for a wide range of particle sizes and velocities. In addition to this behavior, the weight loss due to erosion was found to be strongly dependent on impingement angle. Further, the velocity dependence changed with the impingement angle. In all cases studied the maximum weight loss occurred at approximately 20 degrees.

By assuming that the erosion process is dependent on two mechanisms; one at low angle impingement; one at high angles of attack; and a combination of the two at intermediate approach angles, the relationship for erosion damage may be expressed as follows.

$$\epsilon = K_1 f(\beta_1) (V_{1T}^2 - V_{2T}^2) + f(V_{1N}) \quad (1)$$

where:

- ϵ = the erosion damage per unit mass of impacting particles
- K_1 = material constant
- $f(\beta_1)$ = empirical function of particle impact angle
- V_{1T} = tangential component of incoming particle velocity
- V_{2T} = tangential component of rebounding particle velocity
- $f(V_{1N})$ = component of erosion due to the normal component of velocity.

This approach is similar to that taken by Neilson and Gilchrist (16), as it is predominantly an empirical approach yet requires a knowledge of parametric behavior. The first term of this expression predominates at low angles of attack, and the second term predominates at normal impact where the tangential velocity is zero. The small influence of the particle size has been ignored in this analysis.

The equation appears to indicate that the erosion is directly proportional to the kinetic energy of the particle, in direct contradiction to the observed results. Further, the two terms of $f(\beta_1)$ and $f(V_{1N})$ are not fully described and the calculation of V_{2T} is well beyond the current state of knowledge. An explanation of these items is contained in the following section.

A. Erosion at Low Angles of Attack

At low angles of attack the erosion can be approximated by:

$$\epsilon_1 = K_1 f(\beta_1) [V_{1T}^2 - V_{2T}^2] \quad (2)$$

By defining the tangential restitution ratio as:

$$R_T = \frac{V_{2T}}{V_{1T}} \quad (3)$$

we can write:

$$\epsilon_1 = K_1 f(\beta_1) V_{1T}^2 [1 - R_T^2] \quad (4)$$

or in terms of the approach velocity vector

$$\epsilon_1 = K_1 f(\beta_1) V_1^2 \cos^2 \beta_1 [1 - R_T^2] \quad (4a)$$

The experimental data obtained by the author (48) indicates that the tangential restitution ratio is dependent on the particle velocity (V_1). The data from this reference is plotted in Figure 15. In correlating this limited data, use was made of the theoretical analysis of Sheldon and Kanhere (21). This analysis shows that the depth of penetration of a particle into a surface is linearly proportional to the normal velocity component. It would then be expected that the tangential restitution ratio would have the same linear dependence. Using a linear relationship with the data given in Figure 15, the following equation is obtained for 2024 aluminum alloy.

$$R_T = 1 - 0.0016 V_1 \sin \beta_1 \quad (5)$$

Substituting Equation (5) into Equation (4) gives the following result for a given angle of attack:

$$\epsilon_1 = K V_1^2 [1 - (1 - 0.0016 V_1 \sin \beta_1)^2] \quad (6)$$

where

$$K = K_1 f(\beta_1) \cos^2 \beta_1$$

at a given value of β_1 .

Using this analysis, where the restitution coefficient is a function of the particle velocity, Equation (1), which was developed assuming that the erosion was linearly proportional to the particle kinetic energy loss at impact, is now dependent on a power of velocity greater than two. The calculated results of this equation, for a 20 degree impact angle, are plotted in Figures 6 and 8 along with the experimentally determined results. These analytically determined results accurately predict the velocity dependence of the experimental data, which was taken over a range of velocities from 200 to 600 ft/sec. These results are quadratic in terms of V^2 , however they appear to be linear in terms of $V^{2.8}$ over the interval of interest.

The effect of the angle of impingement (β_1) on erosion is not as easily resolved. Not only does the parameter $f(\beta_1)$ have to be determined, but the experimental data reported by the authors in Reference 48 indicates that the restitution ratio is a stronger function of the angle of attack than Equation (5) predicts. The development of a regular ripple pattern on the surface of the material, also a function of the angle of attack, might account for this.

For this reason, the effect of the particle approach angle is lumped into one parameter, $f(\beta_1)$, and a strictly empirical approach is used to predict its behavior. The results of this analysis yields the following expression.

$$f(\beta_1) = [1 + CK (K_{12} \sin 2 \beta_0)]^2 \quad (7)$$

where:

β_0 = angle of attack where maximum erosion occurs,

$$CK = \begin{cases} 1 & \beta_1 \leq 2 \\ 0 & \beta_1 > 2 \end{cases}$$

K_{12} = material constant.

B. Erosion at Normal Impact

The mechanism of ductile erosion at normal impact cannot be determined using a fundamental cutting or scratching mechanism since there is no velocity component tangential to the surface. The theoretical analyses developed to date have not had much success in predicting this value. Finnie's fundamental analysis (11) predicts that no erosion will occur at normal impact. Bitter (14) predicts that erosion at normal impact will occur as a result of work-hardening of the surface leading to eventual "brittle" failure. This theory is disputed by electron microscope pictures of the eroded surface, which shows the surface material to be deformed by a purely

plastic action. In addition, gold, which exhibits a typical ductial erosion pattern, can absorb enormous amounts of energy when it is beaten into thin sheets of foil. Tilly and Sage (46) proposed that this erosion process could be the result of particle fracture upon impact, with the particle fragments scouring over the surface causing secondary damage. However, for a soft material such as aluminum, it is unlikely that this is the erosion mechanism. Smeltzer, et al. (20) proposed that erosion at normal impact results from particles initially bonding themselves to the material surface, and then being dislodged by further particle impacts. As the particle dislodges, it carries with it a portion of the surface material. This explanation is very plausible, however, the analytical model resulting from this analysis is essentially a curve fit and incorrectly relates the erosion to the square of the velocity. Finally, Finnie (47) proposed that the mechanism causing this erosion could result from one or a combination of the following items:

- a) A roughening of the surface such that the particles strike the surface locally at a variety of angles.
- b) The particles have an initial rotation which is removed upon impact, thereby removing material.
- c) Multiple impacts, battering the surface back and forth, eventually produce fracture by low-cycle fatigue.

The authors (48) investigated the process of the normal impact of erosive particles using high speed photography. The results of this research showed that the particles rebound at angles other than 90 degrees. The amount that a particle deviates from the normal as it rebounds was found to vary over a wide range of values with the average being approximately 26 degrees. This data would seem to substantiate Finnie's hypothesis relating erosion at normal impact to the roughened surface condition.

Thus, even though much experimental information has been obtained on normal erosion, an understanding of the basic mechanisms are not yet agreed upon. Any analysis of these mechanisms would therefore have to resort to curve fitting the data, which is a technique utilized in this analysis.

The component of erosion resulting from normally impacting particles was obtained from the data given in Figures 7 and 9, and is expressed as:

$$f(V_{1n}) = K_3 (V_1 \sin \beta_1)^4 \quad (8)$$

C. Prediction of Erosion of 2024 Aluminum Alloy

Reviewing the previous development, the erosion of 2024 aluminum alloy can be determined by utilizing the following expression:

$$\epsilon = K_1 f(\beta_1) V_1^2 \cos^2 \beta_1 [1 - R_T^2] + f(V_{1n}) \quad (1a)$$

where

$$R_T = 1 - 0.0016 V_1 \sin \beta_1 \quad (5)$$

$$f(\beta_1) = [1 + CK (K_{12} \sin 2 \beta_0)]^2 \quad (7)$$

$$f(V_{1n}) = K_3 (V_1 \sin \beta_1)^4 \quad (8)$$

The empirical constants for quartz impacting the aluminum alloy are:

$$K_1 = 3.67 \times 10^{-6}$$

$$K_{12} = 0.585$$

$$K_3 = 6.0 \times 10^{-12}$$

Figure 16 illustrates the predicted erosion using this equation for different velocities and angles of attack.

The parametric behavior of alumina particles is identical to the quartz particles with the exception of the magnitude of the erosion produced. Thus the material constants for alumina were obtained by directly ratioing the material constants which are:

$$K_1 = 5.32 \times 10^{-6}$$

$$K_{12} = 0.585$$

$$K_3 = 9.0 \times 10^{-12}$$

The predicted results of these equations are plotted with the experimentally obtained data in Figure 5. From this figure it may be observed that the predicted results closely approximate the experimental results. Finally, Figure 17 illustrates predicted erosion for alumina particles using Equation (1) for different velocities and impact angles.

SUMMARY AND CONCLUSIONS

Erosion data was obtained in a unique erosion test facility which was designed in such a manner that the aerodynamics over the test sample are an integral part of the test parameters. The data obtained from this research has been used to develop an analytical model to predict the erosion of 2024 aluminum alloy. This model takes into account a large number of parameters, and was successfully compared to the experimental data. The particle approach angle influences the erosion rate in a very peculiar manner, as it was found that the maximum erosion rate occurs at 20 degrees, whereas only a residual amount of erosion results from normal impact. One very significant finding of this research was that a velocity exponent can be predicted using particle rebound data. Previous models have not been able to predict this parameter. The specimen width affects the erosion rate in that a wider specimen tends to reduce the erosion parameter. The reason for this is not clear at this time.

REFERENCES

1. H. Wahl and F. Hartstein, "Strahlerschleiss," Franckh'sche Verlagshandlung, Stuttgart, 1946.
2. E. Siebel and H.C. Brockstedt, Verschleissminderung, "Maschinenbau" 20 (1941) 457.
3. K. Wellinger and H.C. Brockstedt, "Versuche zur Ermittlung des Verschleisswiderstandes von Werkstoffen für Blasversatzsohr sowie des Einflusses der Rohrverlegung bei Blasversatzanlagen," Gluckauf, 78 (1942) 130.
4. K. Wellinger and H.C. Brockstedt, "ermittlung des Verschleisswiderstandes von Werkstoffen für Blasversatzrohe," Stahl und Eisen, 62 (1942) 635.
5. K. Wellinger, "Sandstrahlverschleiss an Metallen," Z. Metallkunde, 40 (1949) 361.
6. K. Wellinger and H. Uetz, "Verschleissuntersuchungen an Gummi," Z. Ver. deut. Ingr., 96 (1954) 43.
7. K. Wellinger and H. Uetz, "Gleitverschleiss, Spülverschleiss, Strahlverschleiss unter der Wirkung von Kornigen Stoffen," VDI Forschungsheft, (1955) 449; Weat I (1957/58) 225.
8. V.N. Kascheev, "Destruction of a metal surface as a function of the angle of impact of abrasive particles," Zhur. Tehk. Fiz., 25 (1955) 2365.
9. R.L. Stoker, "Erosion Due to Dust Particles in a Gas Stream," Industrial and Engineering Chemistry, Vol. 41, No. 6 (June, 1949).
10. W. A. Stauffer, "Wear of Metals by Sand Erosion," Metals Progress, Vol. 69 (1956) 102.
11. I. Finnie, "The Mechanism of Erosion of Ductile Metals, 1958 Proceedings of Applied Mechanics (ASME), p. 527-532.
12. I. Finnie, "An Experimental Study on Erosion," Proceedings of the Society for Experimental Stress Analysis, Vol. XVII No. 2, 65-70.
13. I. Finnie, "Erosion of Surface by Solid Particles," Wear, 3 (1960) 87-103.
14. J.G.A. Bitter, "A Study of Erosion Phenomena," Part I, Wear, 6 (1963) 5-21.
15. J.G.A. Bitter, "A Study of Erosion Phenomena," Part II, Wear, 6 (1963) 169-190.

16. J.H. Neilson and A. Gilchrist, "Erosion by a Stream of Solid Particles," *Wear*, 11 (1968) 111-122.
17. I. Finnie and Y.H. Kabil, "On the Formation of Surface Ripples during Erosion," *Wear*, 8 (1968) 60-69.
18. G.L. Sheldon and I. Finnie, "The Mechanism of Material Removal in the Erosive Cutting of Brittle Materials," *Journal of Engineering for Industry (ASME)*, Nov., 1966, 393-400.
19. W.J. Head and M.E. Harr, "The Development of a Model to Predict the Erosion of Materials by Natural Contaminants," *Wear*, 15 (1970) 1-46.
20. C.E. Smeltzer, M.E. Gulden, S.S. McElmury, W.A. Compton, "Mechanism of Sand and Dust Erosion in Gas Turbine Engines," USAAVLABS Technical Report 70-36, August 1970.
21. G.L. Sheldon and A. Kanhere, "An Investigation of Impingement Erosion Using Single Particles," *Wear* 21 (1972) pp. 195-209.
22. J.N. Goodier, "On the Mechanics of Indentation and Cratering in Solid Targets of Strain Hardening Metal by Impact of Hard and Soft Spheres," *Pulter Res. Lab. TR 002-64*, Stanford Res. Inst., Menlo Park, California, 1964.
23. A. Thiruvengadam, "The Concept of Erosion Strength," *Hydro-nautics, Inc.*, Technical Report 233-9, Dec. 1965.
24. E. Kreigel, "Der Strahlverschleiss von Werkstoffen," *Chemie-Ingenieur-Technik*, Vol. 40, 1968, p. 31.
25. H.C. Duffin, "A Laboratory Scale Study of Erosion and Deposition due to Gas Borne Solids," *National Gas Turbine Establishment Report M 341*, August, 1960.
26. J.E. Montgomery and J.M. Clark, Jr., "Dust Erosion Parameters for a Gas Turbine," *SAE Summer Meeting Preprint 538A*, Society of Automotive Engineers, New York, 1962.
27. W.A. Hibbert, "Helicopter Trials Over Sand and Sea," *Journal of the Royal Aeronautical Society*, Vol. 69 (Nov. 1965) 769-776.
28. G.V. Bianchini and R.B. Koschman, "T63 Engine Sand and Dust Tolerance Development and Field Experience," *Sixth Conference and Environmental Effects on Aircraft and Propulsion Systems*, Princeton, New Jersey, 1966.
29. J.M. Dent, "Ground Erosion Effects in the Operation of Jet Lift Aircraft," *Sound Vib.* (1966) 4 (3), pp. 259-267.
30. W.J. Head, T. Pacala, and J. Poole, "The Allison-Purdue Dust Technology Program," presented at the *Man-Mobility-Survivability Forum*, April 11-12, 1967.

31. M.L. Woodward, "British Experience with Propulsive Machinery for Air Cushion Vehicles," ASME Publication 68-FT-36, Jan. 1968.
32. R.M. Wood, "Study-Correlation of Aerodynamic Parameters with Compressor Erosion, Final Report," Allison Division of General Motors, February 28, 1969.
33. G.A. Duke, "Erosion Tests on a Modified Rover Gas Turbine," Australian Defense Scientific Service, Aeronautical Research Laboratories, Note No. A R L/M E 297, 1968 (June).
34. J.H. Neilson and A. Gilchrist, "An Experimental Investigation into Aspects of Erosion in Rocket Motortail Nozzles," Wear, 11 (1968), 123-143.
35. E. Raask, "Turbine Erosion by Ash Impace," Wear, 13 (1969) 301-315.
36. C.D. Wood and P.W. Espenschade, "Mechanisms of Dust Erosion," SAE Summer Meeting, Paper 880, SAE New York, 1964.
37. G.T. Sheldon and I. Finnie, "On the Ductile Behavior Nominally Brittle Materials During Erosive Cutting," Journal of Engineering for Industry (ASME), November, 1966, 393-400.
38. G.L. Sheldon, "Similarities and Differences in the Erosion Behavior of Materials," Journal of Basic Engineering (ASME), Sept. 1970, 619-626.
39. I. Finnie, C. Wolak and Y. Kabil, "Erosion of Metals by Solid Particles," Journal of Materials, Vol. 2, No. 3, Sept. 1967, 682-700.
40. I. Kleis, "Problems Der Bestimmung Des Strahlverschleisses Bei Metallen," Wear, 13 (1969) 199-215.
41. W. Sage and G.P. Tilly, "The Significance of Particle Size in Sand Erosion of Small Gas Turbines," The Aeronautical Journal, Vol. 73 (May, 1969).
42. G.P. Tilly, "Erosion Caused by Airborne Particles," Wear, 14 (1969) 63-79.
43. G.P. Tilly, "Sand Erosion of Metals and Plastics; A Brief Review," Wear 14 (1969) 241-248.
44. J.E. Goodwin, W. Sage, and G.P. Tilly, "Study of Erosion by Solid Particles," Proc. Inst. Mech. Engrs., Vol. 184, Pt. 1, No. 15 (1969-70) 279-292.
45. G.C. Smeltzer, M.E. Gulden and W.A. Compton, "Mechanisms of Metal Removal by Impacting Dust Particles," Journal of Basic Engineering, Sept. 1970, 639-654.

46. G.P. Tilly and W. Sage, "The Interaction of Particle and Material Behavior in Erosion Processes," Wear, 16 (1970), 447-465.
47. I. Finnie, "Some Observations on Erosion," Wear, 19 (1972) 81-90.
48. G. Grant, R. Ball, W. Tabakoff, "An Experimental Study of the Erosion Rebound Characteristics of High Speed Particles Impacting a Stationary Specimen," Technical Report No. 73-36, April 1973, University of Cincinnati.
49. G. Grant, W. Tabakoff, "An Experimental Study of Certain Aerodynamic Effects on Erosion, University of Cincinnati, Technical Report No. 73-28, Cincinnati, Ohio, July 1972.
50. G. Grant, W. Tabakoff, "A Quasi-Analytical Method for the Calculation of Particle Trajectories," University of Cincinnati, Technical Report No. 73-35, Cincinnati, Ohio, March 1973.

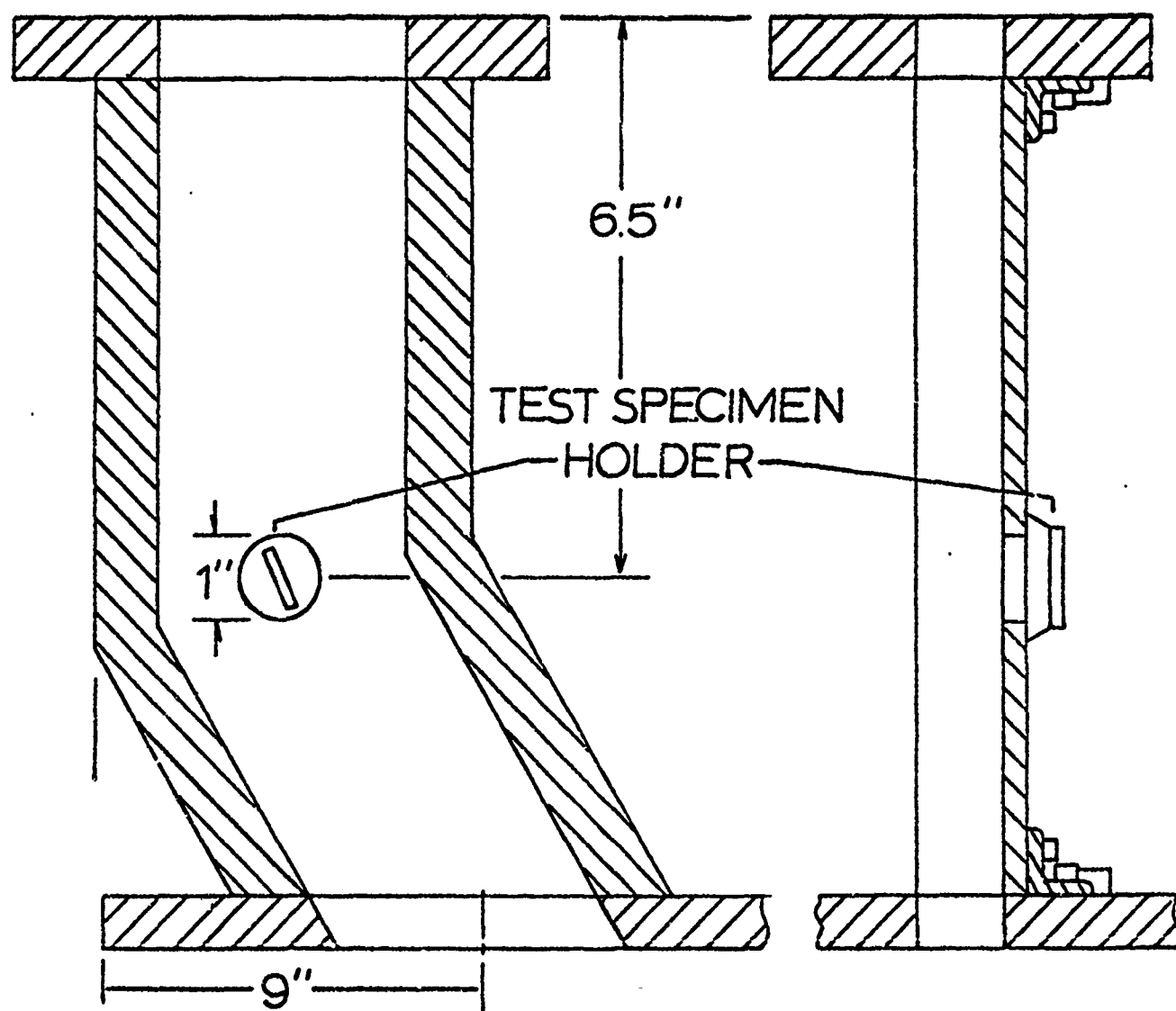


FIG. 2 TEST SECTION
EROSION RESEARCH FACILITY

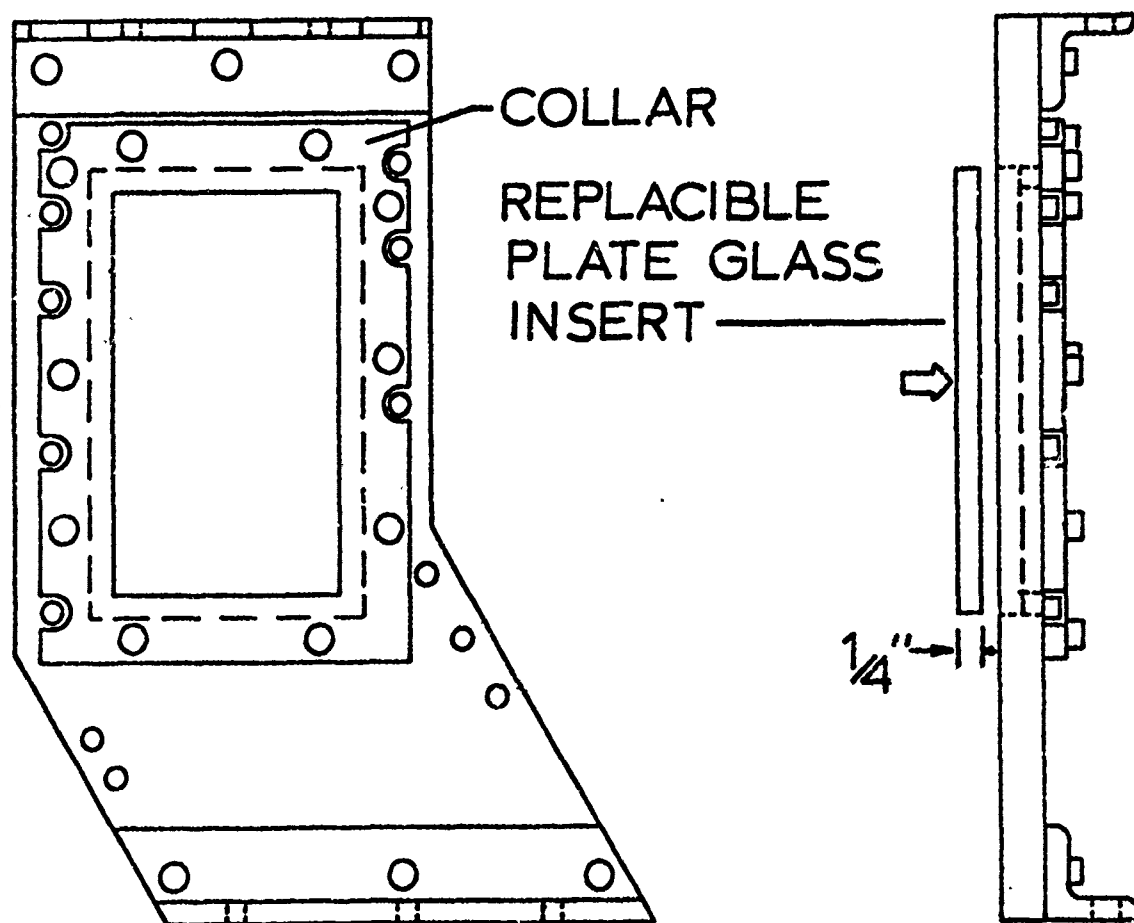


FIG. 3 TEST SECTION PHOTOGRAPHIC INSERT
EROSION RESEARCH FACILITY

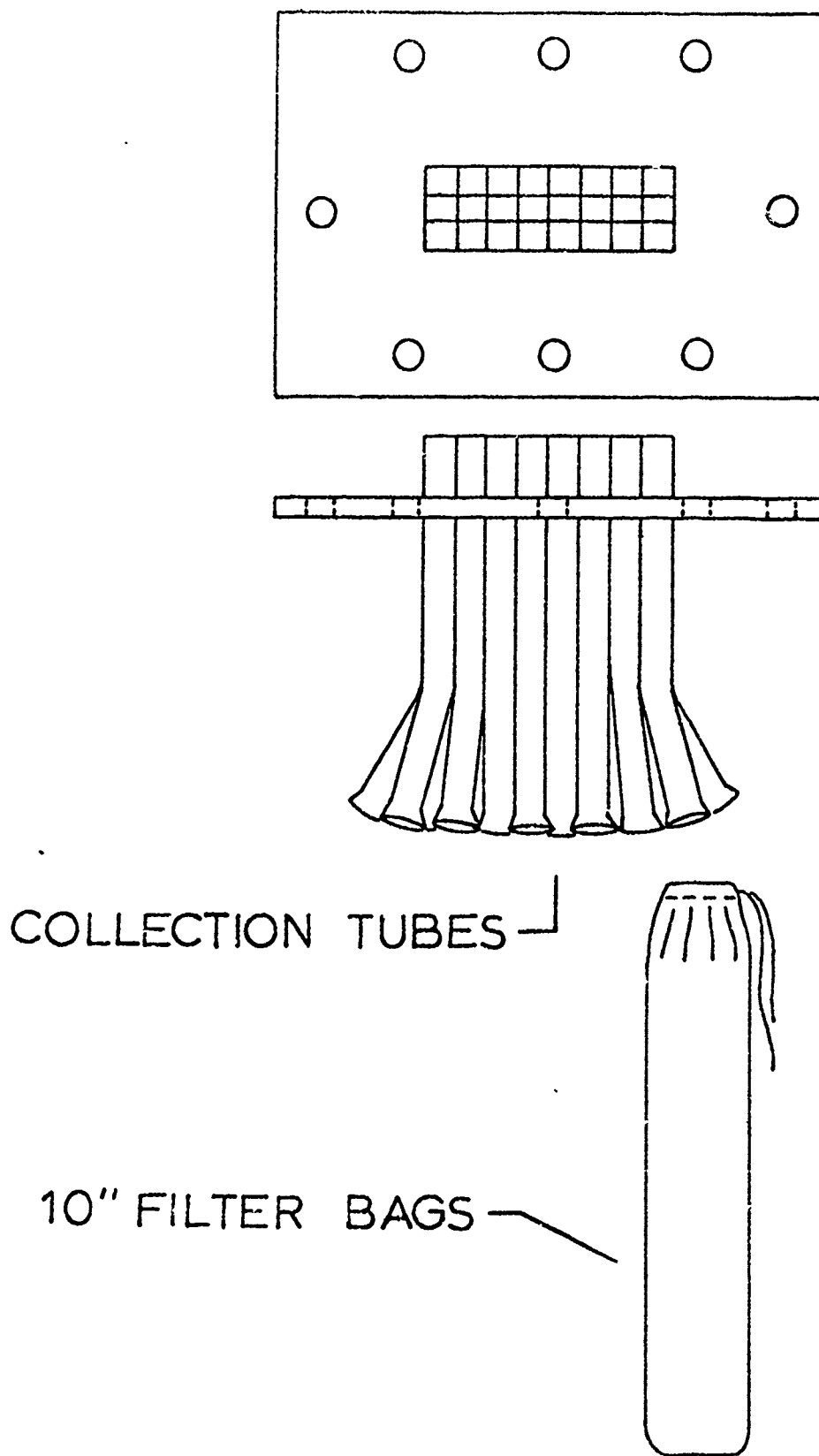


FIG. 4 PARTICLE DISTRIBUTION
ANALYZER
EROSION RESEARCH FACILITY

TARGET MATL - 2024 ALUMINUM

PARTICLE MATL - ALUMINA

PARTICLE SIZE - 110 MICRONS

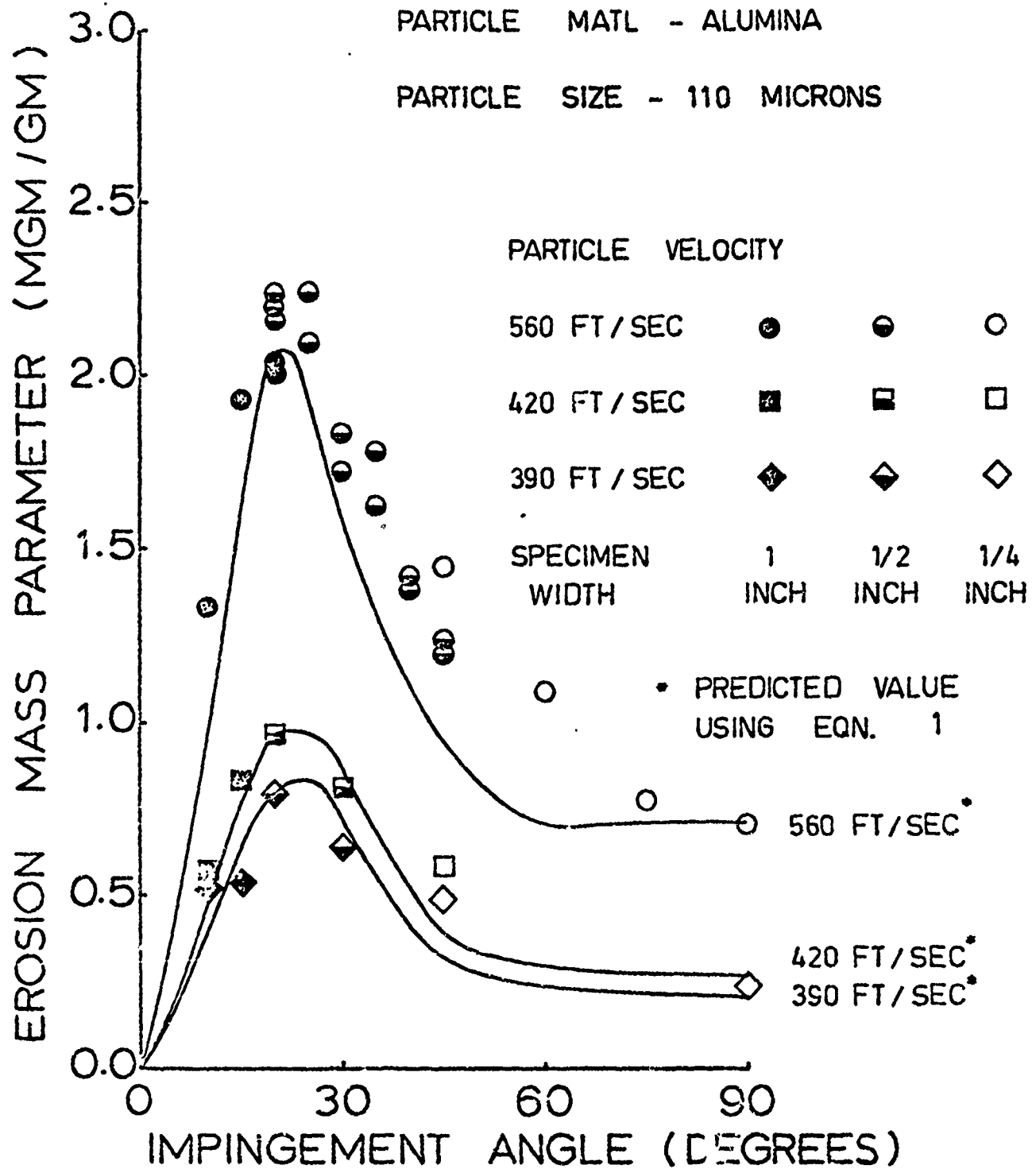


FIG. 5 EXPERIMENTAL AND PREDICTED EROSION RESULTS

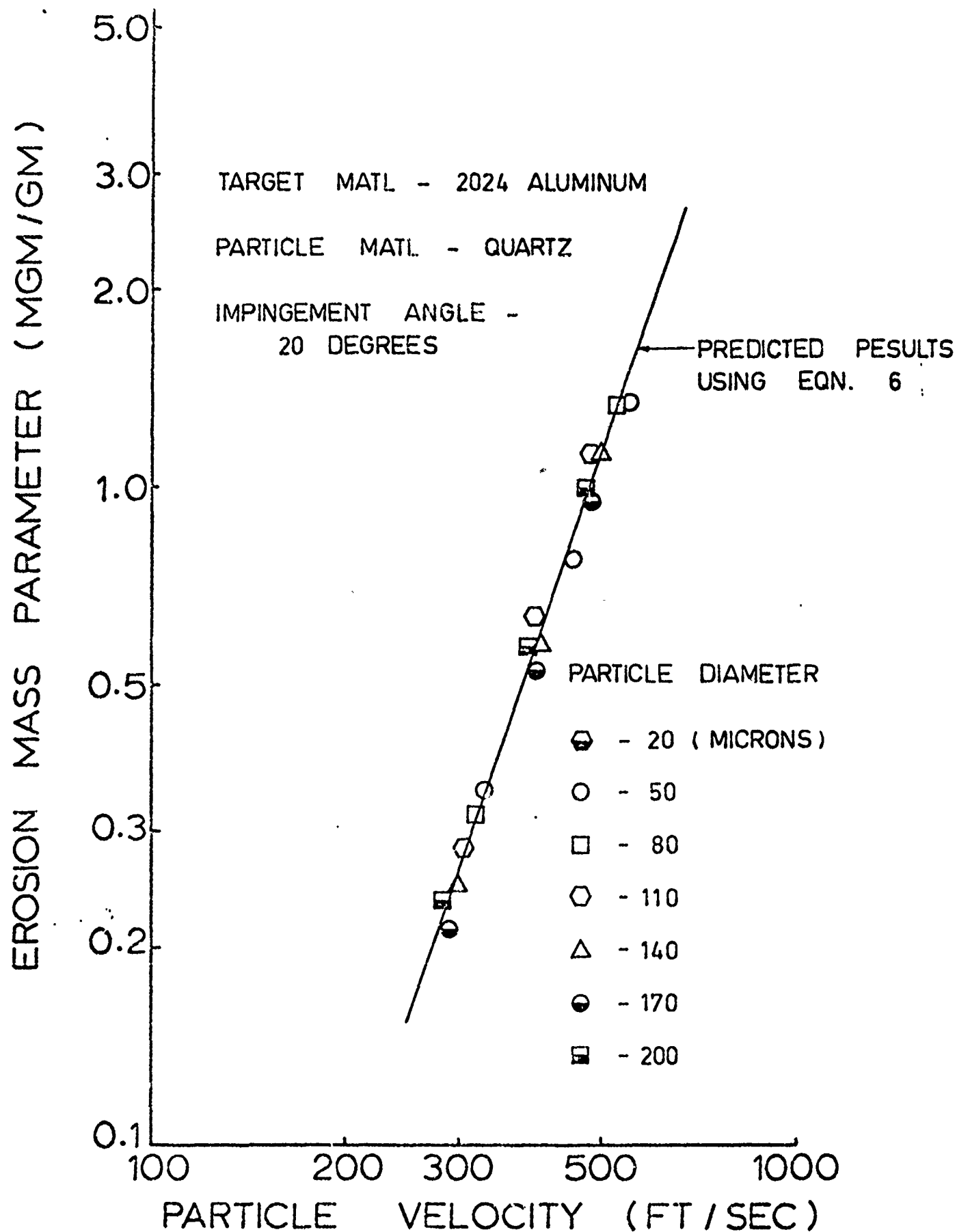


FIG. 6 EFFECT OF VELOCITY ON EROSION RATE

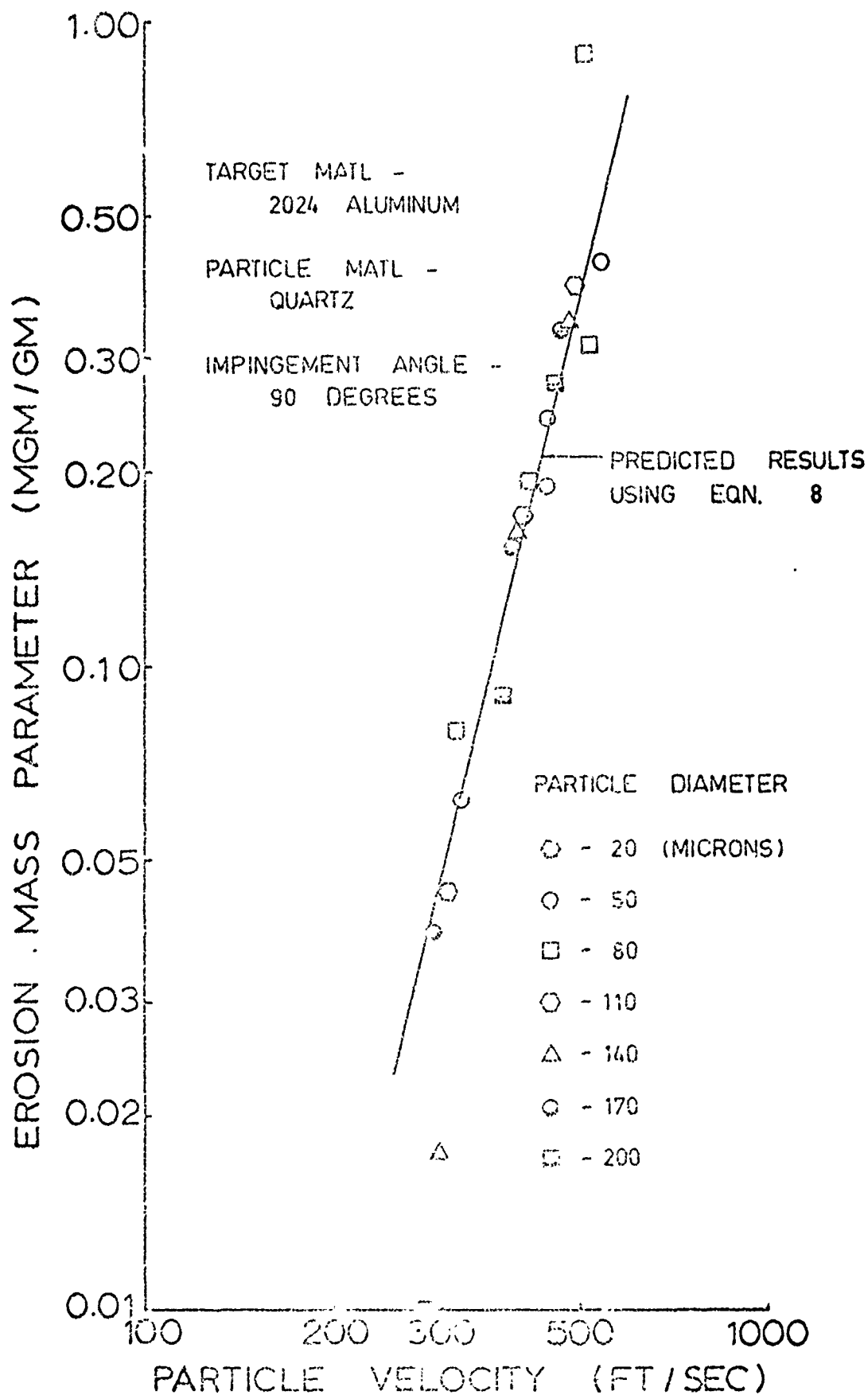


FIG. 7 EFFECT OF VELOCITY ON
EROSION RATE

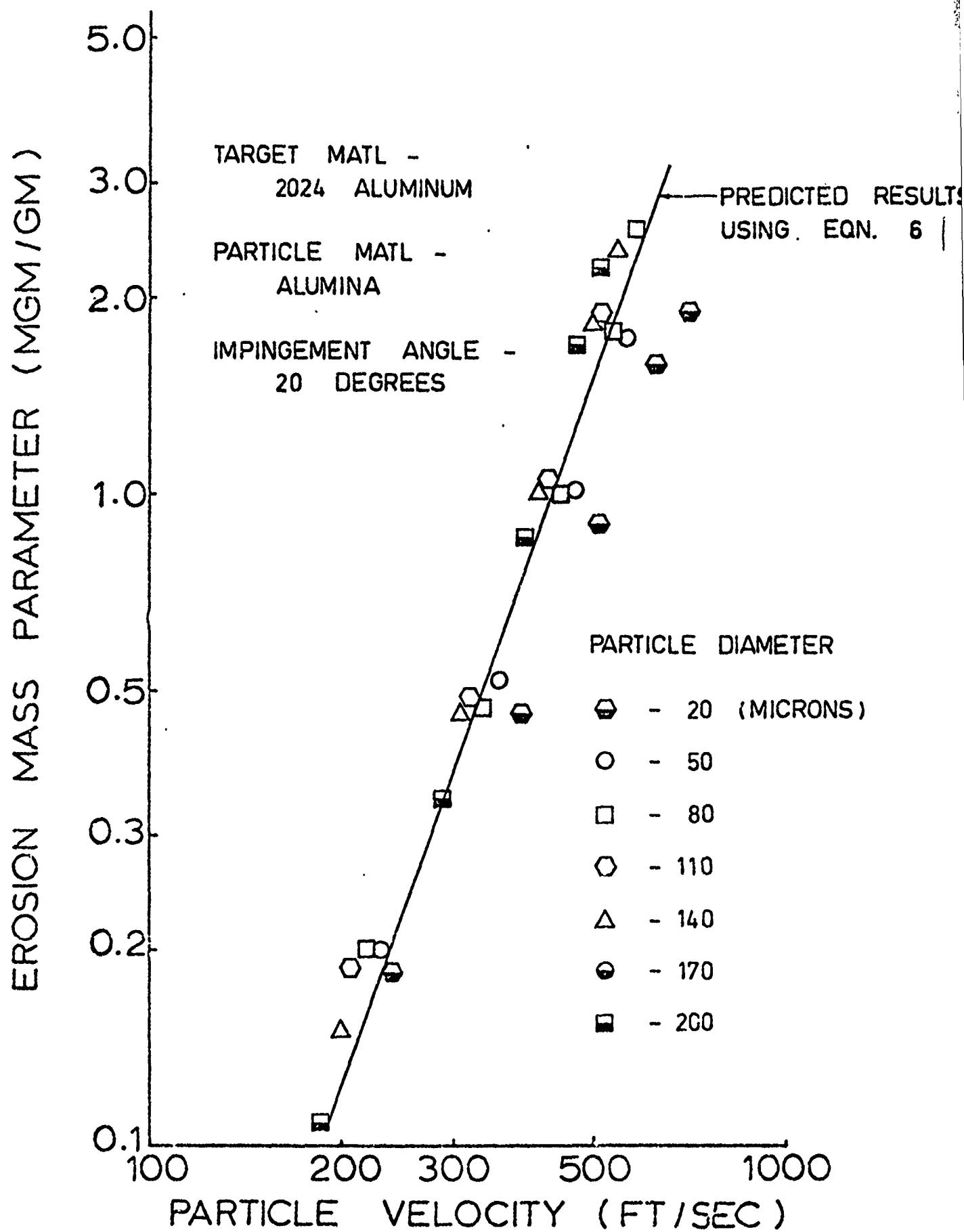


FIG. 8 | EFFECT OF VELOCITY ON
 EROSION RATE

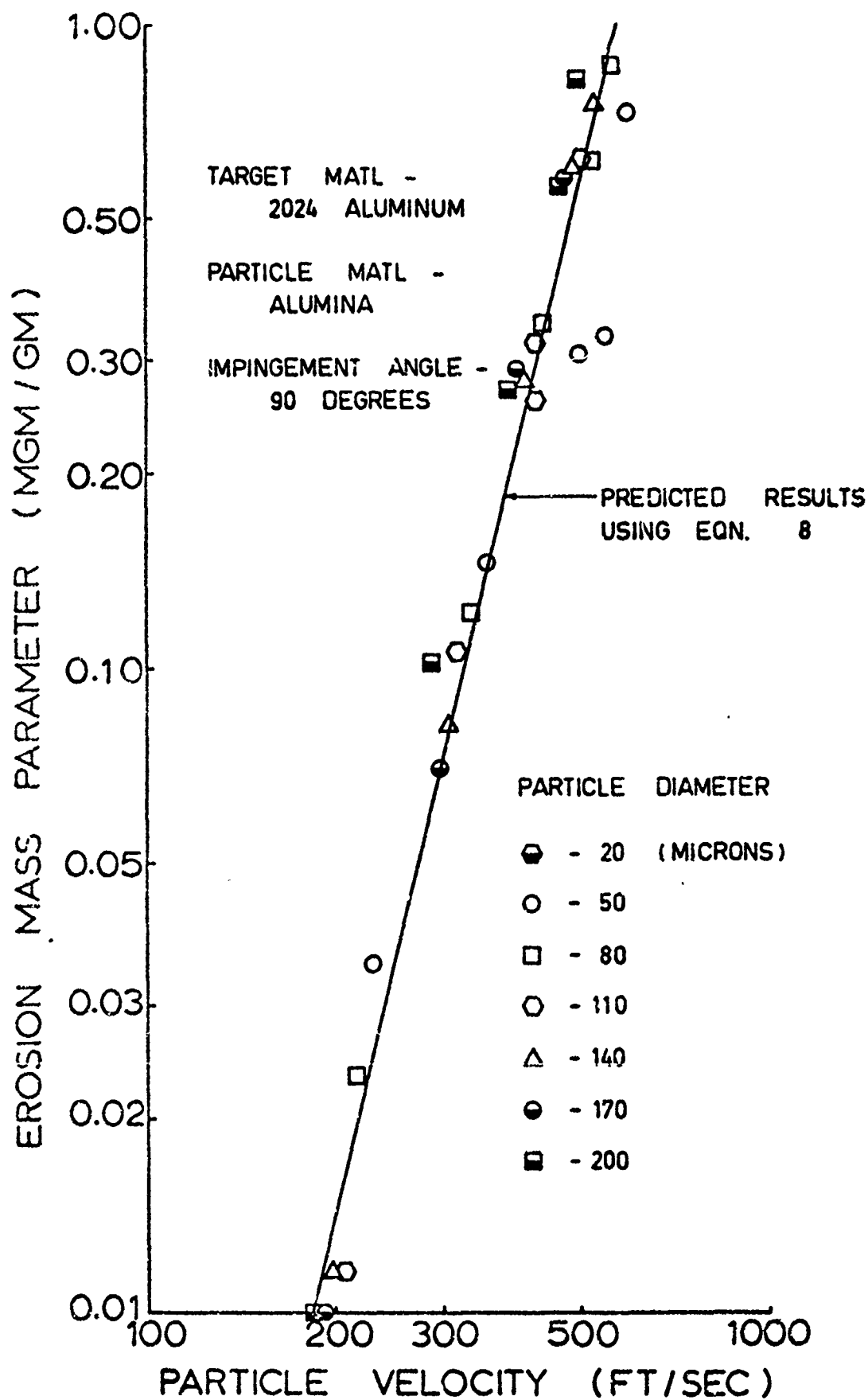


FIG. 9 EFFECT OF VELOCITY ON
EROSION RATE

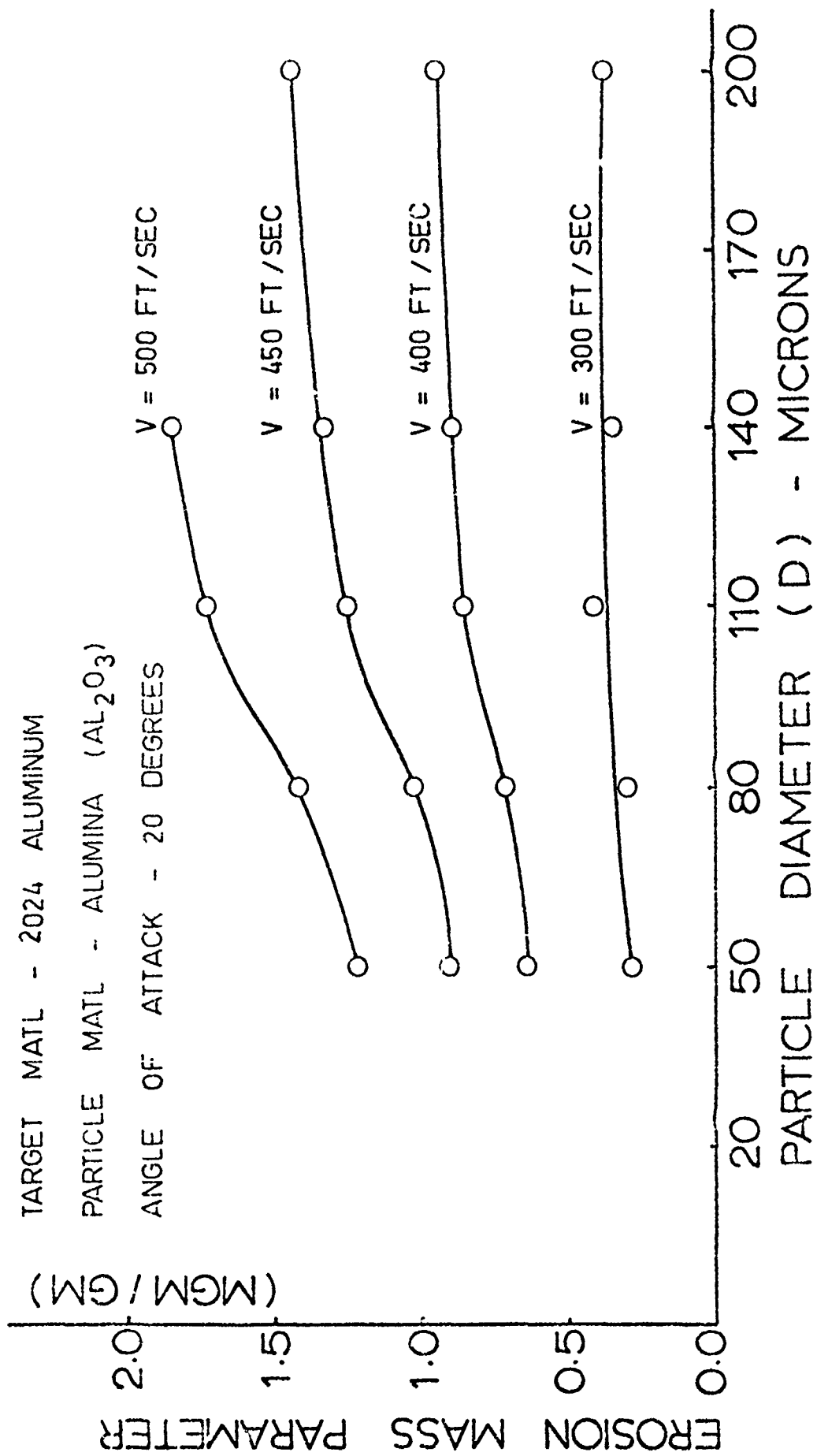


FIG. 10 EFFECT OF PARTICLE DIAMETER ON EROSION

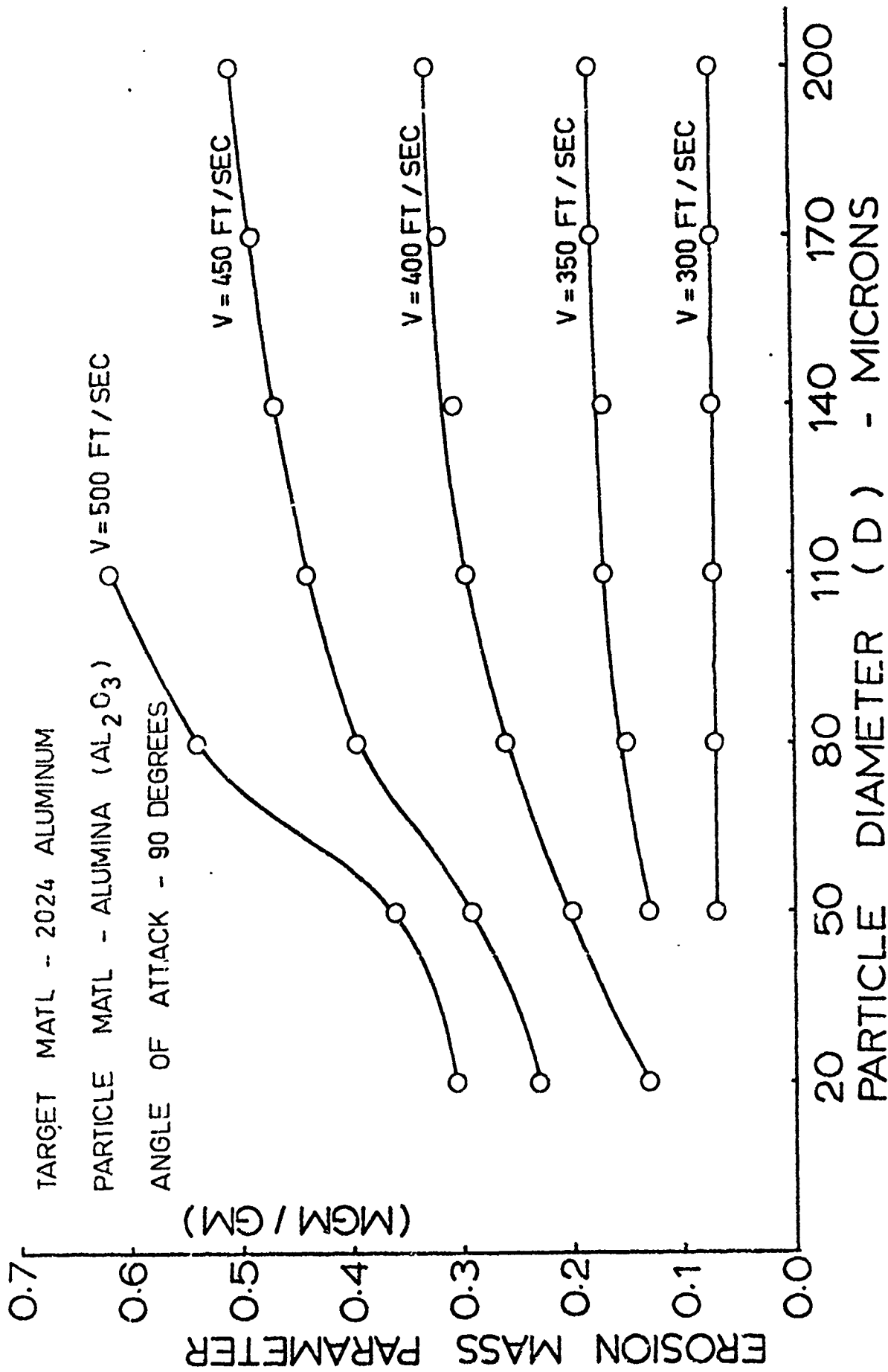


FIG. 11 EFFECT OF PARTICLE DIAMETER ON EROSION

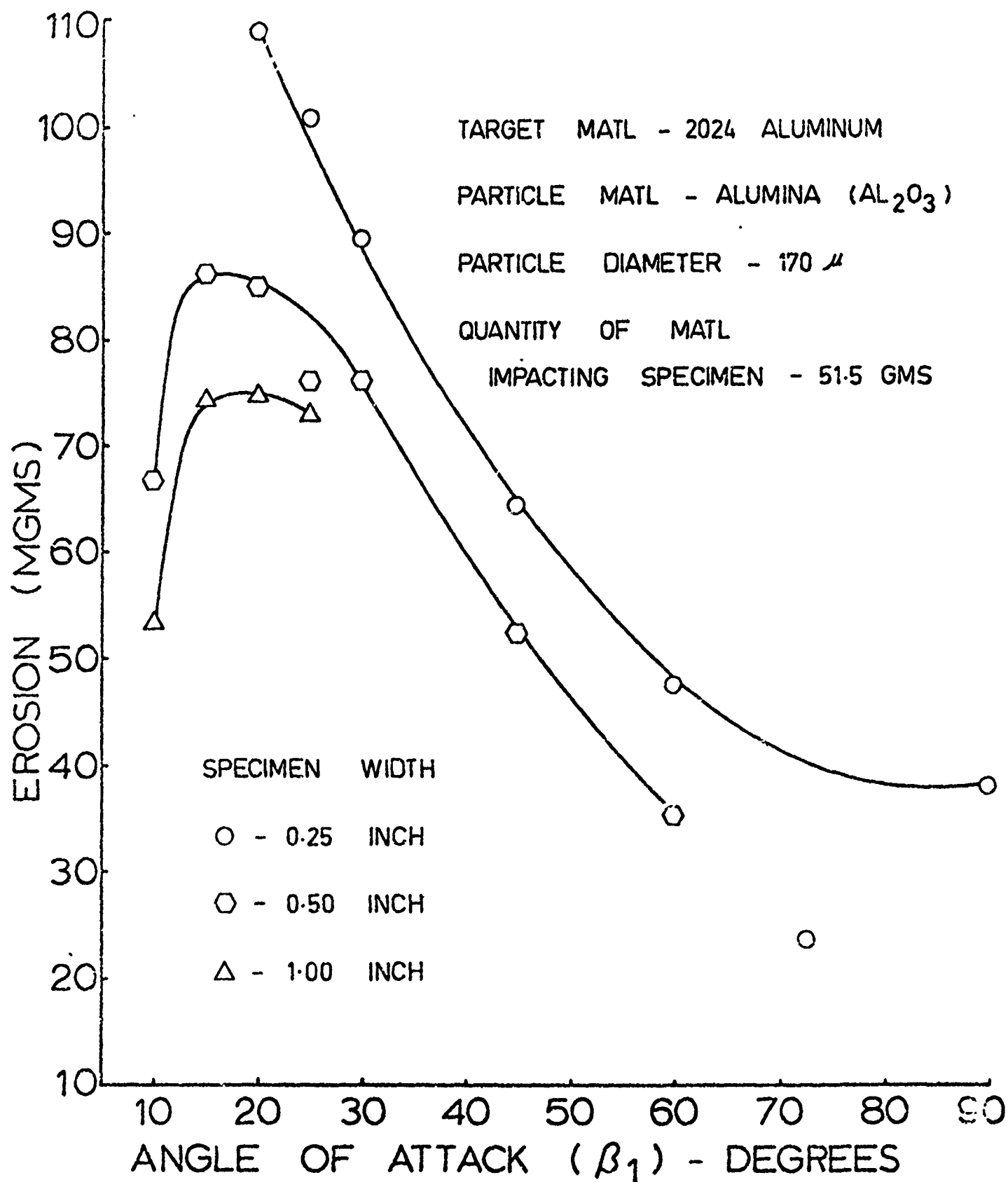


FIG. 12 EFFECT OF SPECIMEN WIDTH ON EROSION

TARGET MATL - 2024 ALUMINUM

VELOCITY

PARTICLE MATL - ALUMINA (Al_2O_3)

O - 540 FT/SEC

PARTICLE DIAMETER - 80 μ

□ - 460 FT/SEC

ANGLE OF ATTACK - 30 DEGREES

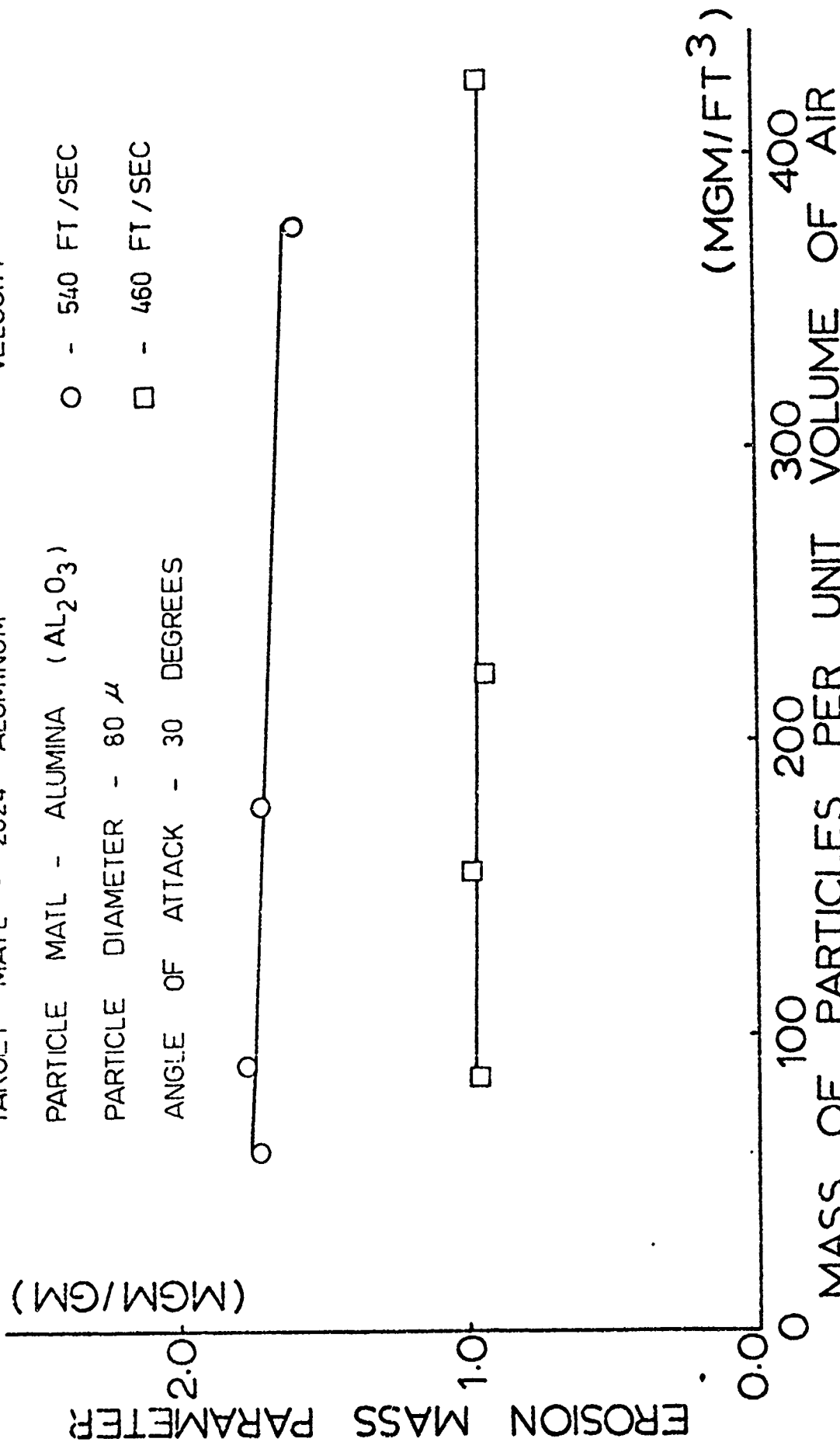


FIG. 13 EFFECT OF PARTICLE MASS CONCENTRATION ON EROSION (MGM/FT³)

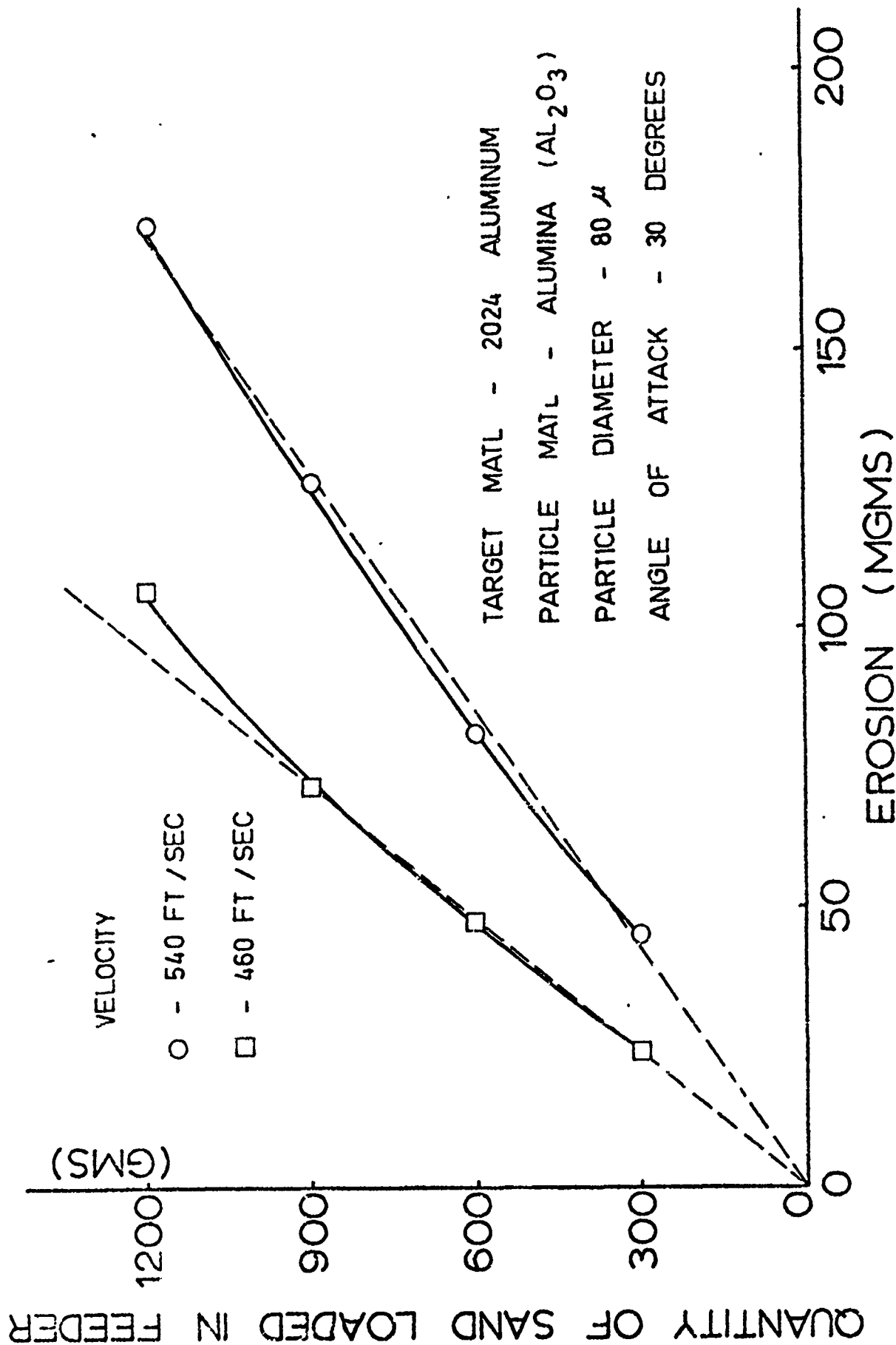


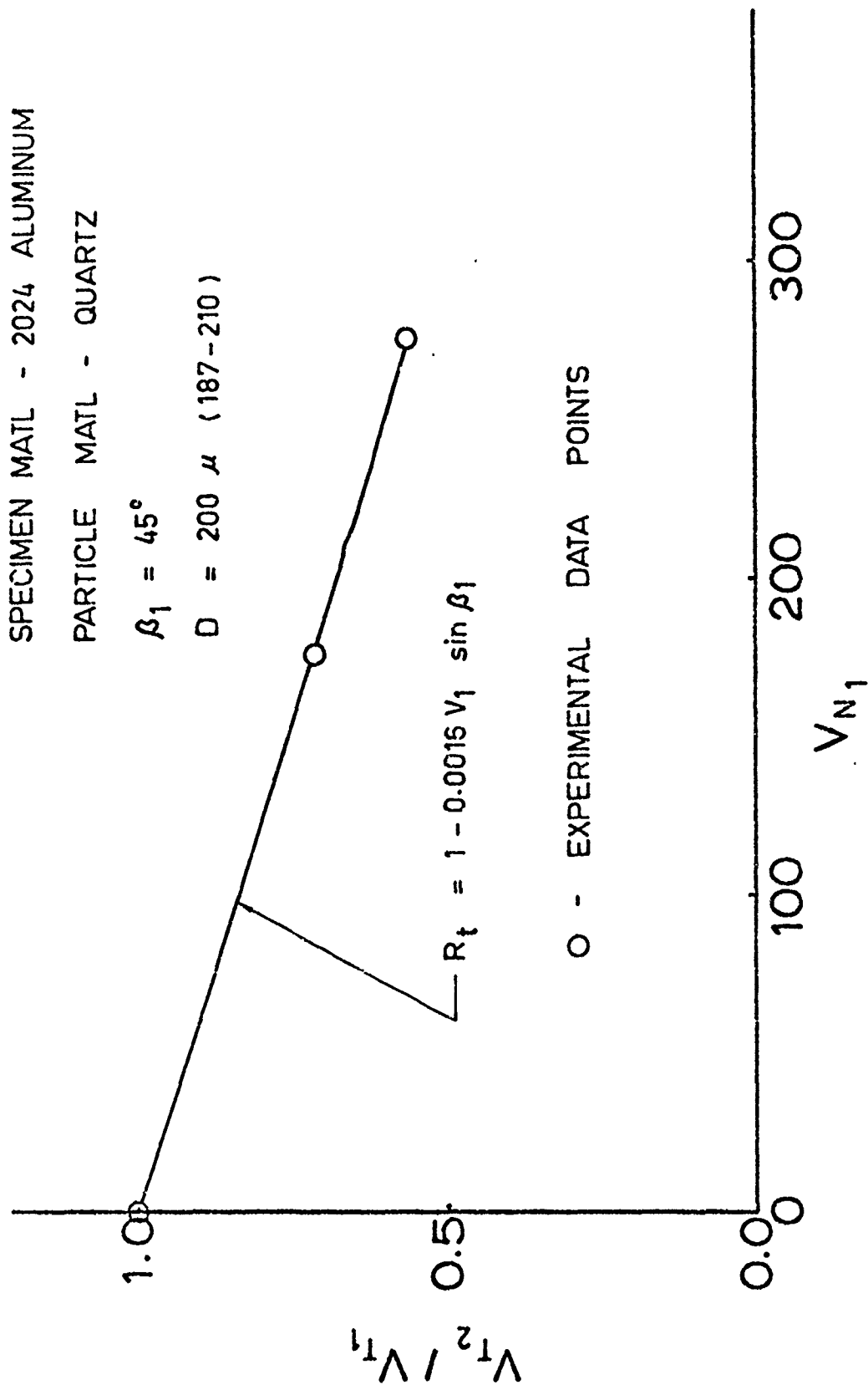
FIG. 14 EROSION vs. QUANTITY OF ABRASIVE USED

SPECIMEN MATL - 2024 ALUMINUM

PARTICLE MATL - QUARTZ

$\beta_1 = 45^\circ$

$D = 200 \mu$ (187-210)



O - EXPERIMENTAL DATA POINTS

FIG. 15 EFFECT OF NORMAL COMPONENT ON TANGENTIAL VELOCITY RESTITUTION RATIO

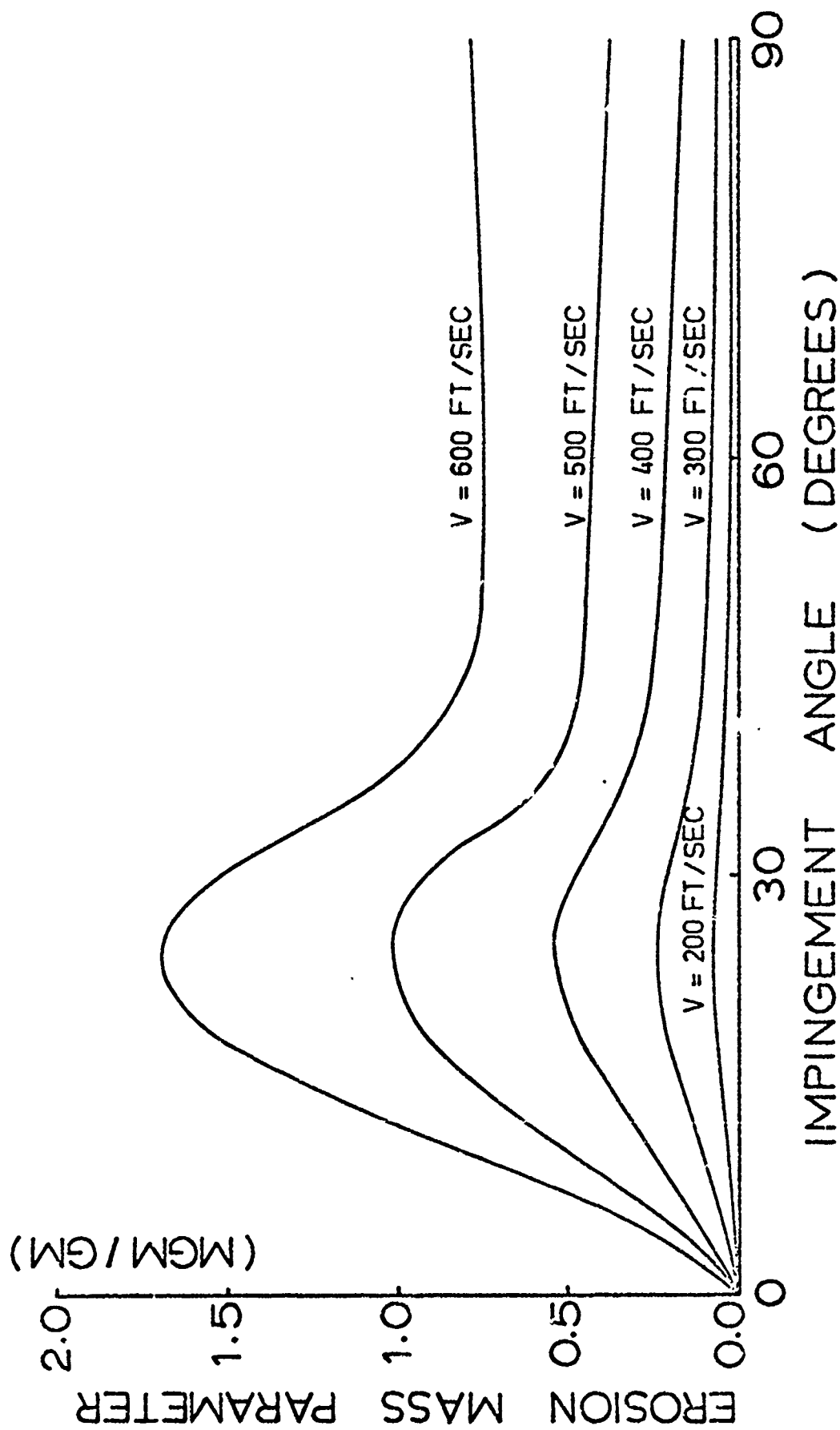


FIG. 16 PREDICTED EROSION FOR 2024 ALUMINUM ALLOY IMPACTED BY QUARTZ SAND DUST

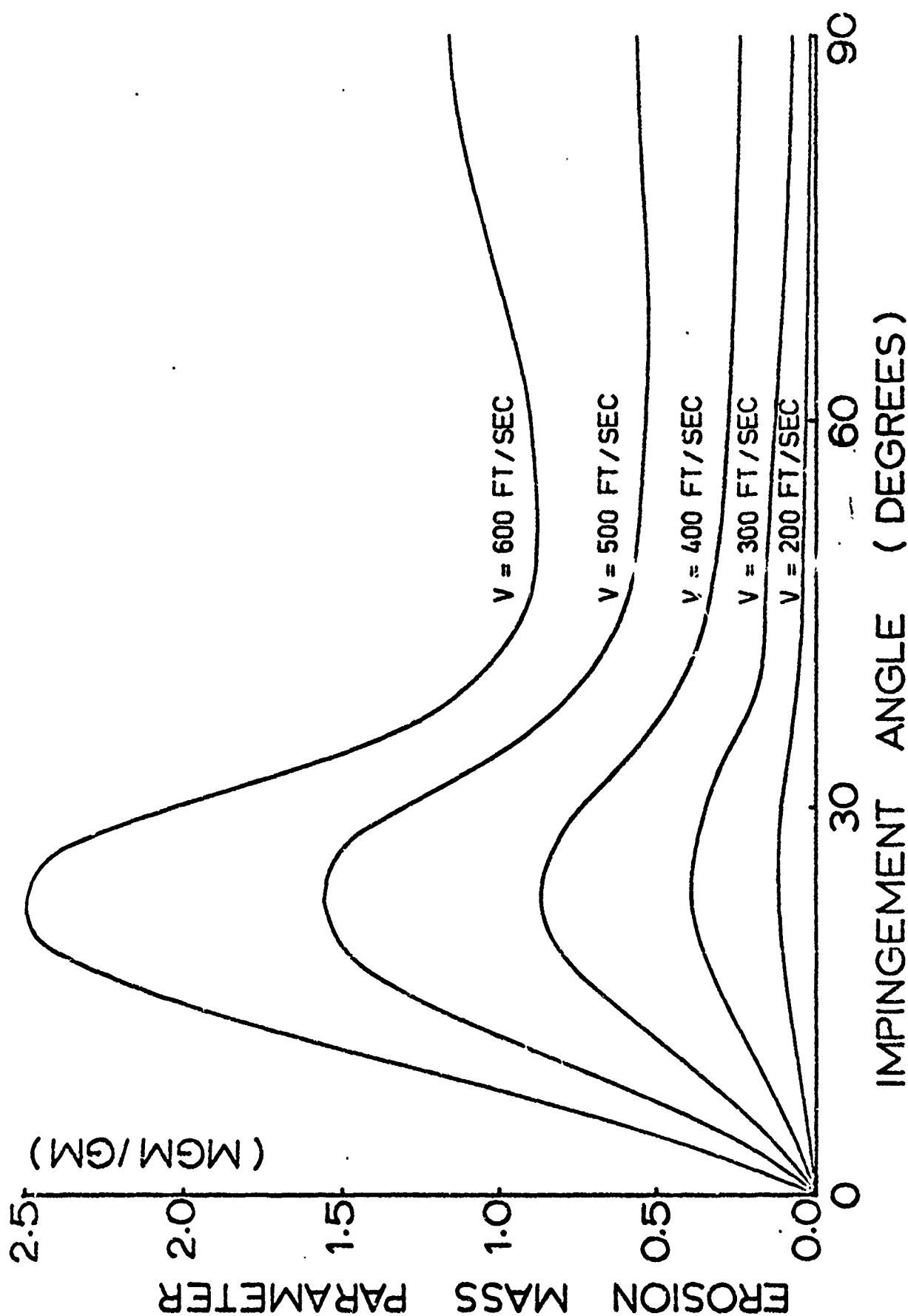


FIG. 17 PREDICTED EROSION FOR 2024 ALUMINUM ALLOY IMPACTED BY ALUMINA SAND DUST